


國立交通大學

光電工程研究所

碩士論文



結合空間及時間多工技術
之新型三維立體顯示器

Spatial-Temporal Hybrid Multi-view 3D Display

研究生：魏景文

指導教授：黃乙白 博士

中華民國九十九年六月

結合空間型及時序型之三維立體顯示器

Spatial-temporal Hybrid Multi-view 3D Display

研究生：魏景文

Student : Ching-Wen Wei

指導教授：黃乙白

Advisor : Yi-Pai Huang

國立交通大學

光電工程研究所

碩士論文

A Thesis

Submitted to Institute of Electro-Optical Engineering

College of Electrical and Computer Engineering

National Chiao Tung University

in partial Fulfillment of the Requirements

for the Degree of

Master

in

Electro-Optical Engineering

June 2010

Hsinchu, Taiwan, Republic of China

中華民國 九十九 年 六 月

結合空間及時間多工技術 之新型三維立體顯示器

碩士研究生：魏景文 指導教授：黃乙白副教授

國立交通大學電機學院 光電工程研究所

摘 要

近幾年來，由於二維顯示器方面技術的成熟，及一般大眾對於影像娛樂需求的提升，立體顯示器已成為目前各大廠商和學術研究的主流，並期望能藉此提供給大眾更真實的視覺感觀效果。在目前的現實生活中，藉由透過觀察者戴眼鏡的技術達到三維視覺效果，已普遍應用在一般商業立體電影院。然而，立體顯示技術如何實現於一般家庭用顯示器，主要還有以下幾點需克服的議題：(一) 如何使觀察者不需戴眼鏡，即可達到近似於日常生活的立體視覺效果。(二) 如何設計整體立體顯示器，在長時間觀看下不會感到不適，並欣賞到高品質的立體畫面。

本篇論文，即在考量解析度、出光效率以及畫面均勻度的情況下，結合空間多工及時間多工型兩種裸眼立體顯示器技術，提出一種新型的裸眼立體顯示器背光，並藉由光學模擬軟體得到最佳化結構參數。最後透過硬體實現，使觀察者在長時間欣賞由該背光系統所提供的立體影像下，不會感到不舒服並欣賞到接近日常視覺的高品質立體影像。

Spatial-Temporal Hybrid Multi-view 3D Display

Student: Ching-Wen Wei Advisor: Dr. Yi-Pai Huang

**Institute of Electro-Optical Engineering
National Chiao Tung University**

Abstract

Currently, stereoscopic displays are widely utilized for entertainment. Nevertheless, 2D multiplexed auto-stereoscopic displays are popular because of multi-view and without wearing eyeglasses, including spatial-multiplexed displays and temporal-multiplexed displays. However, spatial-multiplexed displays present low resolution 3D images and temporal-multiplexed displays produce limited number of views because of LC response time. Therefore, a four-directional temporal backlight was proposed to produce four viewing zones sequentially, including a sequential LED plate, a cylindrical lens, a dual directional prism, and a diffuser. Then, by adding a 240Hz LCD and a multi-views parallax barrier in front of the proposed backlight, a spatial-temporal hybrid 3D display was demonstrated for large panels with wide viewing angle, multi-view, acceptable 3D resolution and light efficiency.

誌 謝

首先，本人在此誠摯的感謝謝漢萍教授和指導老師黃乙白副教授，在碩士的兩年求學生涯中，提供豐富的實驗室資源和良好的研究環境。此外對於研究過程、研討會報告及英文能力的指導鞭策，培養我未來進入公司職場後所應具備的基本條件。也由衷感謝各位口試委員對於本論文所提供的寶貴建議，使整體內容更加趨於完備。

除此之外，特別感謝許精益學長這兩年的教導帶領。無論是對於論文研究方向上給的建議，及遇到問題解決的過程，學長紮實且多元的學歷背景，對於我這兩年的碩士研究有莫大的幫助，也讓我學習到除了光電之外，不同領域的專業知識及科技新知。

感謝王國振、廖凌堯、蔡柏全、王奕智、張育誠、陳致維、蔡韻竹等博班學長姐，提供各方面專業的指導與意見，也感謝宜如、佑禎、拓江、靖堯、博文、俊賢、浩玆、宜伶、高銘、益興等碩班學長姊們，做為下一屆的我們研究及做學問的榜樣。碩二的同學們，期竹、璧丞、裕閔、毅翰、世勛、怡菁、姚順、甫奕、耆賢和泳材，在這兩年中無論是在研究、課業和生活上一起打拼與互相扶持。最後也要向實驗室的張雅惠和李穎佳兩位助理小姐及學弟妹們表達最誠摯的感謝，讓我們做研究之餘沒有後顧之憂，並使實驗室整體像一個大家庭一樣隨時充滿歡愉的氣氛。

最後，對於我的家人及朋友，感謝你們這幾年來背後的支持與鼓勵，使我能考上交大光電工程研究所並順利完成兩年的碩士學位，這份喜悅我將分享給所有認識跟幫助過我的人。

Table of Contents

Abstract (Chinese)	iii
Abstract (English)	iv
Acknowledgement	v
Table of Contents	vii
Chapter 1	1
1.1 Preface.....	1
1.2 Classification of 3D Displays	3
1.3 Motivation and Objectives	4
1.4 Thesis Organization	5
Chapter 2	6
2.1 Criteria of 3D Displays	6
2.1.1 Crosstalk & Average Crosstalk	6
2.1.2 Number of Views & Viewing-Zone Uniformity	7
2.1.3 Voxels and 3D Resolution.....	9
2.1.4 Light Efficiency	10
2.1.5 Image Uniformity.....	11
2.2 Stereoscopic Displays	11
2.3 Auto-Stereoscopic Displays	13
2.3.1 Spatial-Multiplexed 3D Displays.....	13
2.3.2 Temporal-multiplexed 3D Displays	15
2.3.3 Spatial-Temporal hybrid 3D Displays	16
2.4 Summary	17
Chapter 3	19
3.1 Four-Directional Temporal Backlight.....	20
3.1.1 Sequential LED Plate.....	20
3.1.2 Cylindrical Lens.....	21

3.1.3 Dual Directional Prism	22
3.1.4 Diffuser	23
3.2 240Hz LCD	25
3.3 Multi-View Parallax Barrier.....	26
3.4 Summary	27
Chapter 4	29
4.1 Geometric Optics Evaluation of Proposed 3D Backlight	29
4.1.1 Refracted Procedure in Cylindrical lens	29
4.1.2 Refracted Procedure in Prism	30
4.2 Simulations of Four-Directional Temporal Backlight.....	32
4.2.1 Sequential LED Plate	32
4.2.2 Cylindrical Lens.....	34
4.2.3 Dual Directional Prism	36
4.2.4 Diffuser	37
4.3 Summary	39
Chapter 5	40
5.1 Tolerance of the Four-Directional Temporal Backlight	40
5.1.1 Distance between Neighboring LEDs (P).....	40
5.1.2 Divergent Angle of LEDs (Θ).....	42
5.1.3 Curvature Radius of Lens (R)	43
5.1.4 Distance between Lens and LEDs (D).....	44
5.1.5 Obtuse angle of dual directional prism (A).....	45
5.2 Demonstration of Four-Directional Temporal Backlight	46
5.3 Spatial-Temporal Hybrid Multi-View 3D Display.....	48
Chapter 6	51
6.1 Conclusions.....	51
6.2 Future Works	52
References	57

Figure Captions

Fig. 1-1 Stereoscopic display and auto-stereoscopic display [1].	1
Fig. 1-2 Binocular parallax phenomenon.	2
Fig. 1-3 Definition of perceived depth behind and in front of a display.	2
Fig. 1-4 Motion parallax phenomenon.	3
Fig. 1-5 Classification of 3D displays.	4
Fig. 2-1 Definition of crosstalk and average crosstalk.	7
Fig. 2-2 3D images with and without crosstalk [5].	7
Fig. 2-3 4-views 3D displays.	8
Fig. 2-4 Definition of viewing-zone uniformity.	8
Fig. 2-5 High and low resolution images.	9
Fig. 2-6 Diagram of voxel and perceived depth[6].	9
Fig. 2-7 Relation between pixel disparity, perceived depth, and number of voxels [6].	10
Fig. 2-8 Transmittance of each element in LCD [7].	10
Fig. 2-9 Measuring points for image uniformity.	11
Fig. 2-10 Diagram of shutter eyeglasses 3D displays.	12

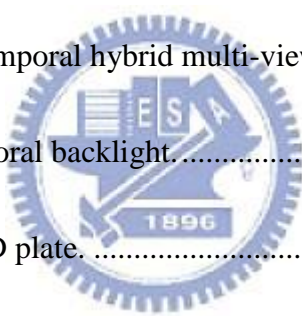

Fig. 2-11 Diagram of polarized eyeglasses 3D displays.	12
Fig. 2-12 Spatial-multiplexed 3D displays	14
Fig. 2-13 Design equations of multi-view parallax barrier.	14
Fig. 2-14 Design equations of multi-view cylindrical lens.....	15
Fig. 2-15 Side-emission sequential backlight 3D displays.	16
Fig. 2-16 Time division parallax barrier high resolution auto-stereoscopic display....	16
Fig. 2-17 2D backlight and 3D backlights.	17
	
Fig. 3-1 Structure of spatial-temporal hybrid multi-view 3D display.....	19
Fig. 3-2 Four-directional temporal backlight.....	20
Fig. 3-3 240Hz sequential LED plate.	21
Fig. 3-4 Diagram of cylindrical lens.	22
Fig. 3-5 Diagram of dual directional prism.	23
Fig. 3-6 Diagram of diffusers.....	24
Fig. 3-7 Definitions of transmittance and haze.	25
Fig. 3-8 Diagram of four-directional temporal backlight and 240Hz LCD.	26
Fig. 3-9 Multi-views parallax barrier diagram.....	26
Fig. 3-10 Light distribution of spatial-temporal hybrid multi-view 3D display.	27

Fig. 4-1 Refraction from air to the cylindrical lens.	30
Fig. 4-2 Refraction from the cylindrical lens to air.....	30
Fig. 4-3 Refraction from air to the prism.....	31
Fig. 4-4 Refraction from the prism to air.	31
Fig. 4-5 Parameters of sequential LED plate.	32
Fig. 4-6 Hot spots phenomenon.....	33
Fig. 4-7 Comparisons between white LEDs built using LighTools 6.1.....	33
Fig. 4-8 Two parameters in cylindrical lens.....	34
Fig. 4-9 Angular difference vs. Distance between lens and LEDs (D) as R=10mm. ..	35
Fig. 4-10 Five cylindrical lens samples after optimization.....	35
Fig. 4-11 Diagram and parameters of dual directional prism.	36
Fig. 4-12 Refraction on micro prism 1 and micro prism 2.	37
Fig. 4-13 Diagram of Gaussian scattering phenomenon.....	38
Fig. 4-14 Average crosstalk & viewing-zone uniformity vs. α	38
Fig. 4-15 Four-directional temporal backlight light distribution in simulation.	39
Fig. 5-1 Tolerance of distance between neighboring LEDs (P).....	41
Fig. 5-2 Light distributions of P=3mm, 4mm and 5mm.....	41
Fig. 5-3 Light distributions of $\Theta=\pm 12^\circ, \pm 20^\circ$ and $\pm 28^\circ$	42

Fig. 5-4 Tolerance of LEDs divergent angle (Θ).	43
Fig. 5-5 Tolerance of lens curvature radius (R).	43
Fig. 5-6 Light distributions of D=10mm, 12mm and 14mm.	44
Fig. 5-7 Tolerance of distance between lens and LEDs (D).	45
Fig. 5-8 Tolerance of obtuse angle in dual directional prism (A).	45
Fig. 5-9 Light distributions of A=58°, 60° and 62°.	46
Fig. 5-10 Component implementations in four-directional temporal backlight.	47
Fig. 5-11 Light distributions of four-directional temporal backlight.	47
Fig. 5-12 Design of multi-view parallax barrier in the proposed 3D display.	48
Fig. 5-13 Light distributions of spatial-temporal hybrid multi-view 3D display.	49
Fig. 5-14 Fabrication of spatial-temporal hybrid multi-view 3D display.	49
	
Fig. 6-1 Comparisons between simulation and experiment.	53
Fig. 6-2 Vertical crosstalk phenomenon.	53
Fig. 6-3 Solutions to horizontal and vertical crosstalk.	54
Fig. 6-4 Temporal crosstalk in the synchronization between the backlight and LCD.	55
Fig. 6-5 Solutions to the temporal crosstalk phenomenon.	56
Fig. 6-6 Moiré phenomenon caused by the parallax barrier and the LCD.	56

Chapter 1

Introduction

1.1 Preface

Nowadays, display developments are pursued through needing more natural images. Images containing three-dimensional coordinate information are necessary for humans to perceive real life images. In Fig. 1-1, 3D displays, including stereoscopic displays and auto-stereoscopic displays, are the next generation in display technology.



Fig. 1-1 Stereoscopic display and auto-stereoscopic display [1].

The binocular parallax phenomenon and the motion parallax phenomenon cause stereoscopic visions in real life [2]. The binocular parallax phenomenon is that when an observer sees an object, the observer's two eyes receive different 2D images. Then, the brain combines two 2D images to produce stereoscopic visions, as shown in Fig.

1-2. 3D displays utilize the binocular parallax phenomenon to produce the perceived depth defined in Fig. 1-3. A 3D display producing deep perceived depth presents obvious stereoscopic visions.

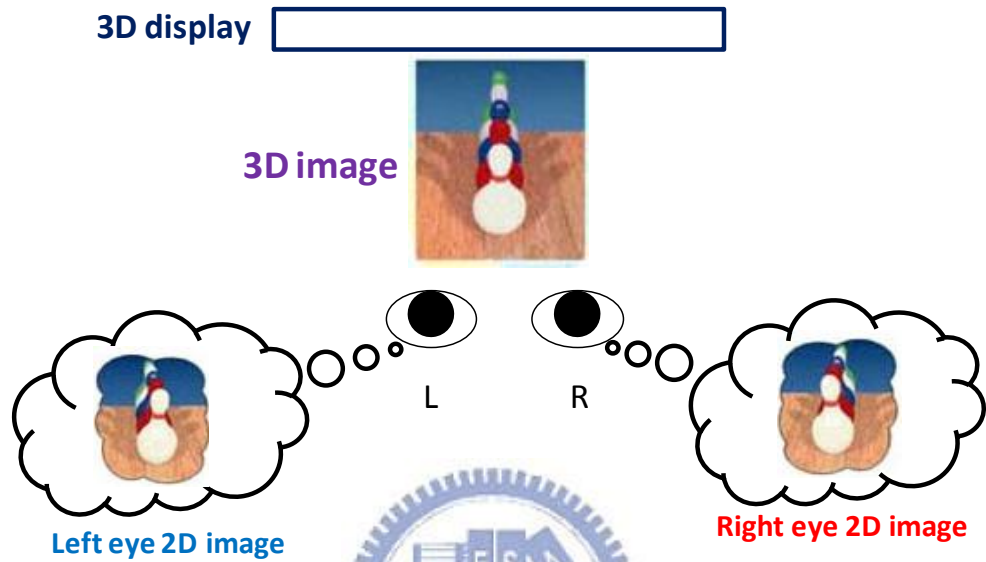


Fig. 1-2 Binocular parallax phenomenon.

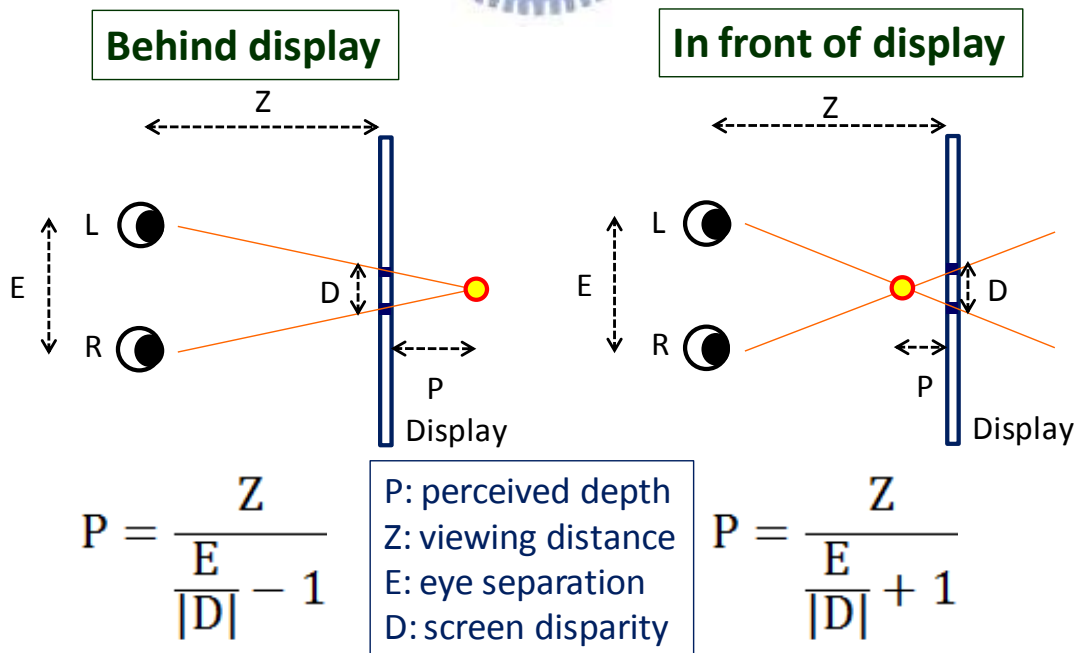


Fig. 1-3 Definition of perceived depth behind and in front of a display.

The motion parallax phenomenon means that when an observer sees an object from different directions, the observer perceives different images continuously. Multi-view 3D displays can produce the motion parallax phenomenon, as shown in Fig. 1-4. A 3D display producing a lot of views presents lifelike 3D images.

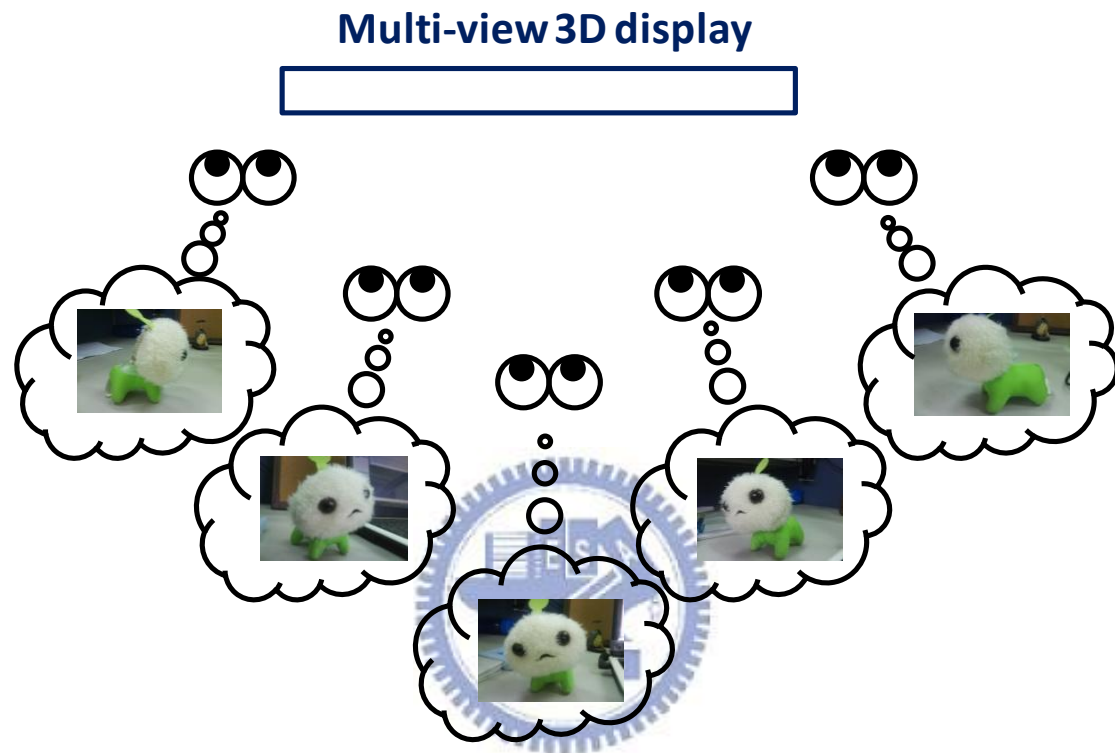


Fig. 1-4 Motion parallax phenomenon.

1.2 Classification of 3D Displays

3D displays include stereoscopic displays and auto-stereoscopic displays. The 3D display classification is shown in Fig. 1-5. Stereoscopic displays include shutter eyeglasses 3D displays and polarized eyeglasses 3D displays. Currently, stereoscopic displays are widely used in cinemas because many people can perceive the same 3D movies simultaneously by wearing eyeglasses. However, wearing eyeglasses and the motion parallax phenomenon are drawbacks in stereoscopic displays. Therefore, auto-stereoscopic displays were developed to introduce 3D techniques into daily life

[3], including Holographic 3D displays and 2D-multiplexed 3D displays. But Holographic 3D displays have color distortion and large recording data requirements in 3D movies. Consequently, 2D-multiplexed 3D displays are attractive because of multi-view, not required eyeglasses, and ease of fabrication.

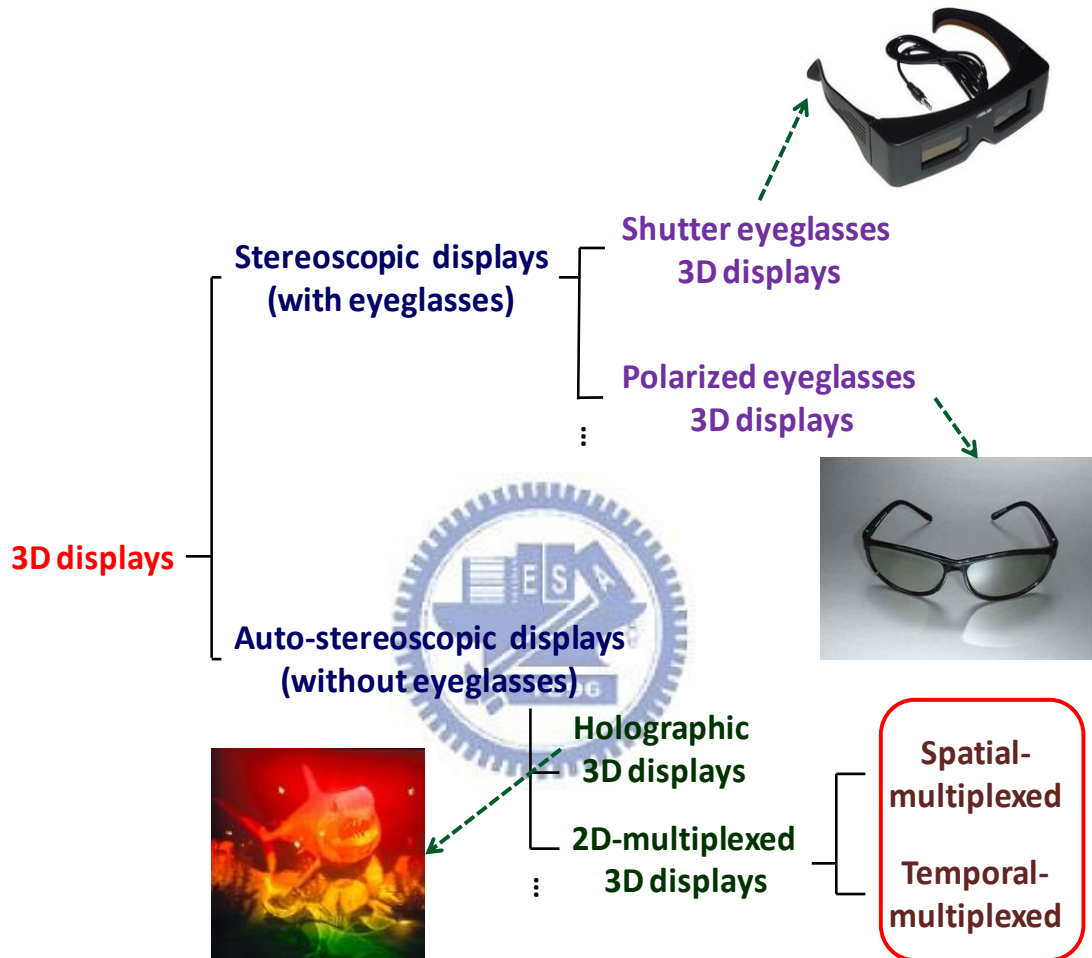


Fig. 1-5 Classification of 3D displays.

1.3 Motivation and Objectives

As mentioned in Sec. 1.2, 2D-multiplexed 3D displays, including spatial-multiplexed 3D displays and temporal-multiplexed 3D displays are popular now. However, spatial-multiplexed 3D displays present low resolution and low light efficiency. Temporal-multiplexed 3D displays produce limited number of views and

non-uniform images in large LCDs. Therefore, a spatial-temporal hybrid multi-view 3D display was proposed to solve drawbacks in spatial-multiplexed and temporal-multiplexed 3D displays.

1.4 Thesis Organization

The thesis is organized as follows: criteria for evaluating 3D displays are defined in **Chapter 2**. Configurations and drawbacks of existing 3D displays are also illustrated. In **Chapter 3**, structure and design of the proposed 3D display are presented. After that, simulation results are analyzed in **Chapter 4** and experimental results are discussed in **Chapter 5**. Finally, conclusions and future works are presented in **Chapter 6**.



Chapter 2

Criteria & Prior Multiplexed 3D Displays

This chapter defines the criteria for evaluating 3D displays. Additionally, configurations, mechanisms, and drawbacks of several representative 3D displays are reviewed and illustrated.

2.1 Criteria of 3D Displays

3D displays are more complex than 2D displays due to the binocular parallax phenomenon and the motion parallax phenomenon. Therefore, some criteria are defined in this section to evaluate 3D displays [4].

2.1.1 Crosstalk & Average Crosstalk

Displaying two different 2D images to the left and right eye causes the binocular parallax phenomenon. However, if the left eye or the right eye receives a wrong image due to light leakage, the brain is confused while combining two 2D images, and observers feel fatigue. Therefore, in multi-view 3D displays, crosstalk and average crosstalk are defined in Fig. 2-1 to evaluate fatigue level. A 3D display with high crosstalk presents distorted 3D images, as shown in Fig. 2-2. The human can tolerate crosstalk below 15% ~ 20%. Consequently, reducing light leakage is essential for 3D displays to present clear 3D images.

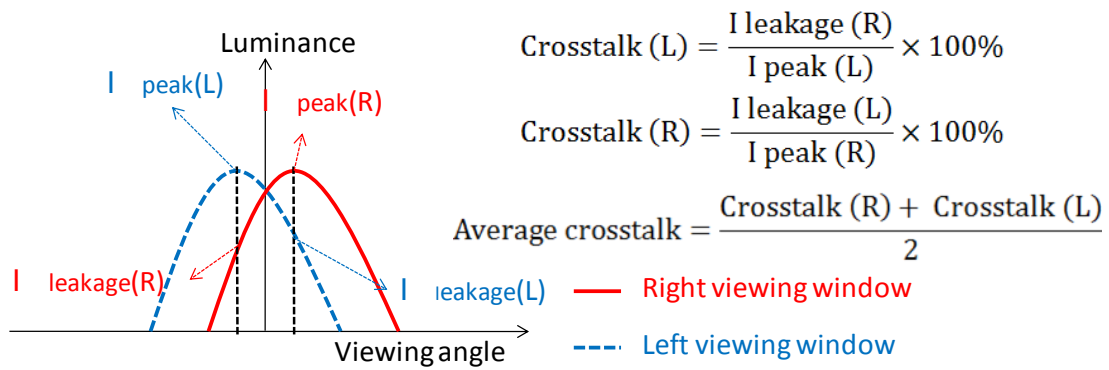


Fig. 2-1 Definition of crosstalk and average crosstalk.

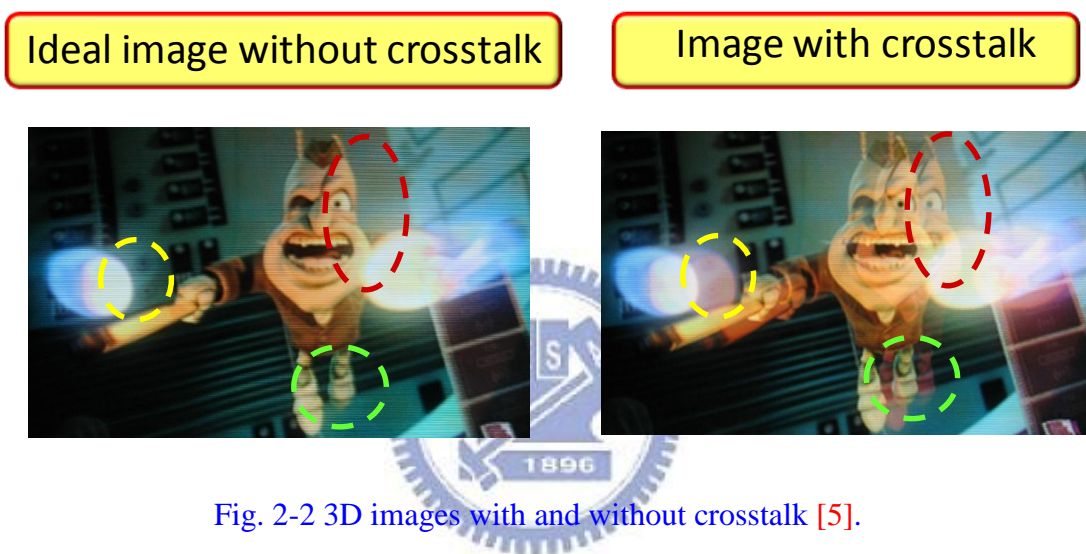


Fig. 2-2 3D images with and without crosstalk [5].

2.1.2 Number of Views & Viewing-Zone Uniformity

A view is the range that an observer's eye can see clear 2D images. The left and right eye receives two different 2D images when the observer sees a 3D image. So a 3D image contains two views. A multi-view 3D display produces different 3D images according to the observer's location, as shown in Fig. 2-3. Therefore, 3D displays producing large number of views present lifelike 3D images. However, in daily life, an object perceived from different directions is continuous. Therefore, the viewing-zone uniformity is defined in Fig. 2-4. If the viewing-zone uniformity is below 70%, an observer perceives dark images while moving to different locations.

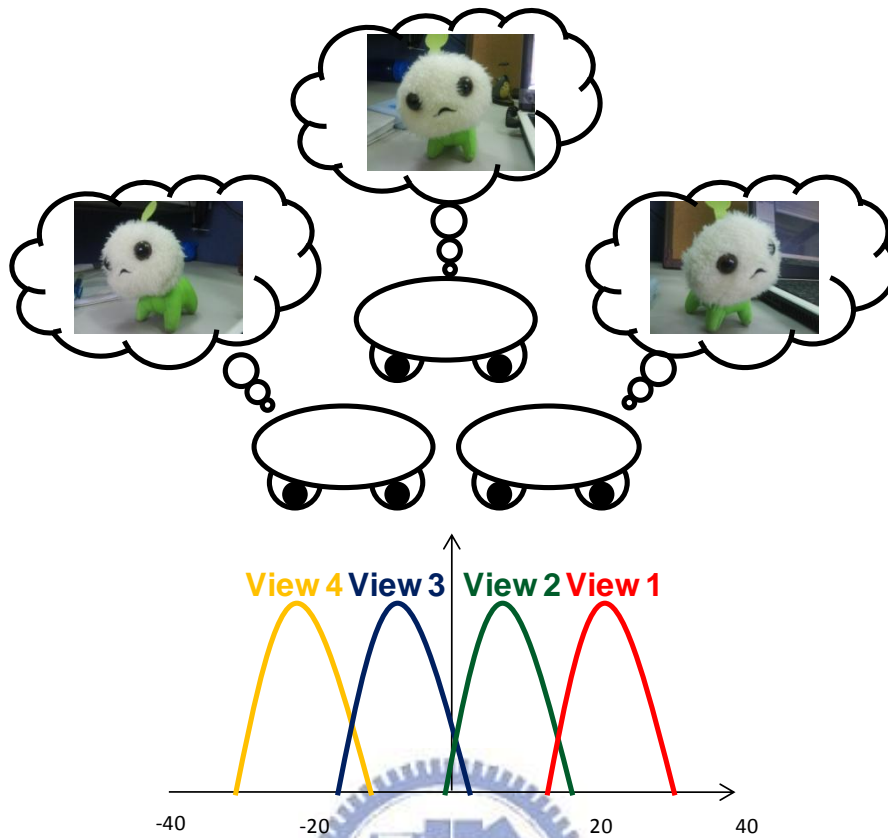
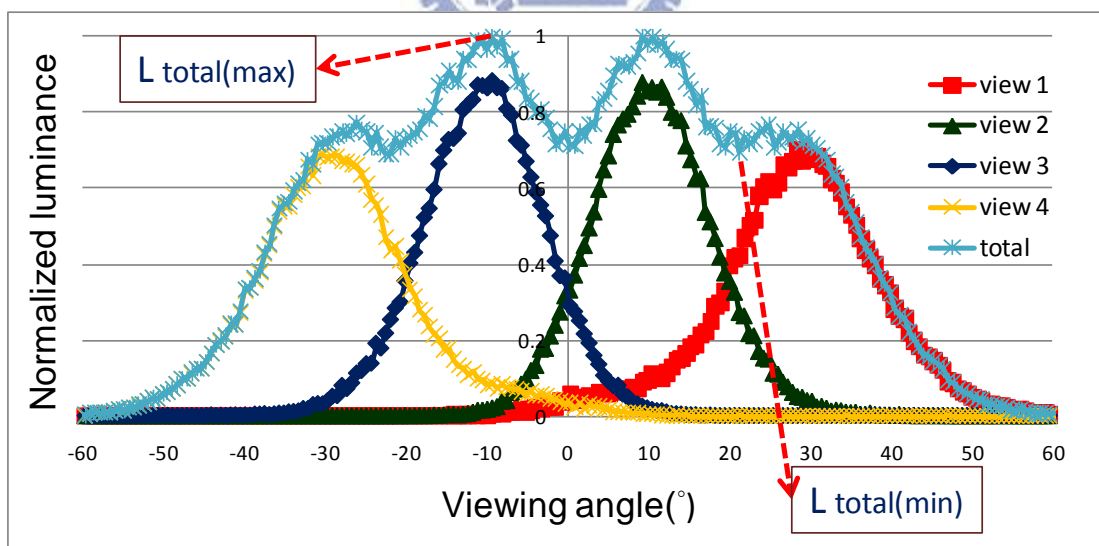


Fig. 2-3 4-views 3D displays.



$$\text{Viewing-zone uniformity} = L_{\text{total (min)}} / L_{\text{total (max)}}$$

Fig. 2-4 Definition of viewing-zone uniformity.

2.1.3 Voxels and 3D Resolution

Display resolution means the number of distinct pixels displayed in an image. In a fixed size 2D display, an image with large number of pixels presents high resolution and clear image contents, as shown in Fig. 2-5. Similarly, in 3D displays, the voxel is a volume of perceived depth produced by a disparity between a left pixel and a right pixel, as shown in Fig. 2-6. In Fig. 2-7, the large pixel disparity produces deep perceived depth but low voxel number and low 3D image resolution. Because two views compose a 3D image, the 2D resolution per view is also a key characteristic in 3D displays. Observers can perceive clear 3D images if the left and right eye receives high 2D resolution per view.

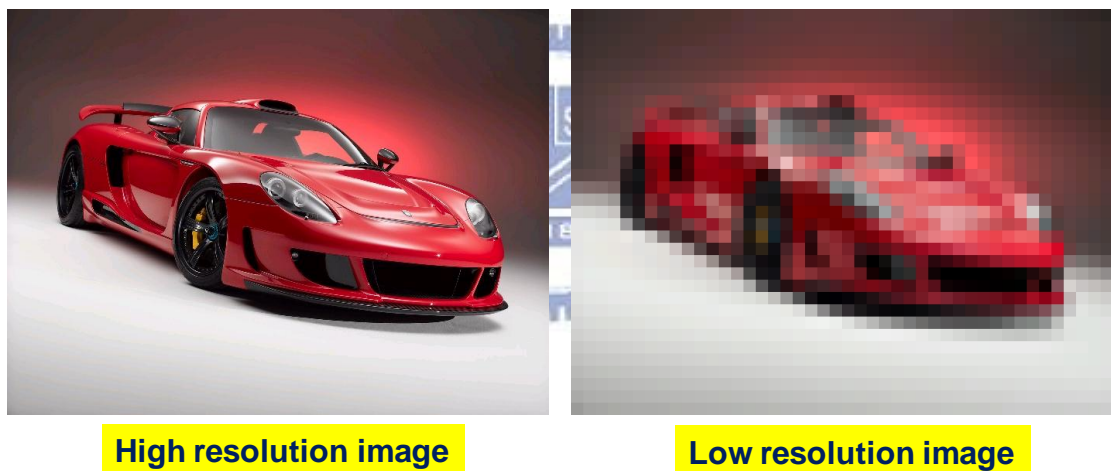


Fig. 2-5 High and low resolution images.

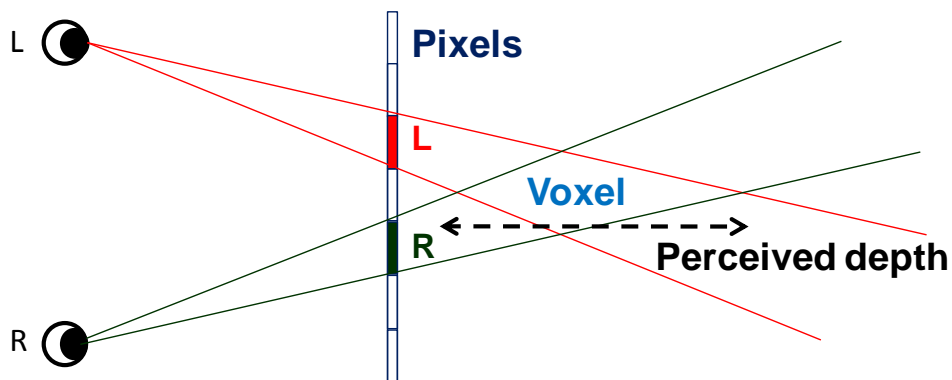
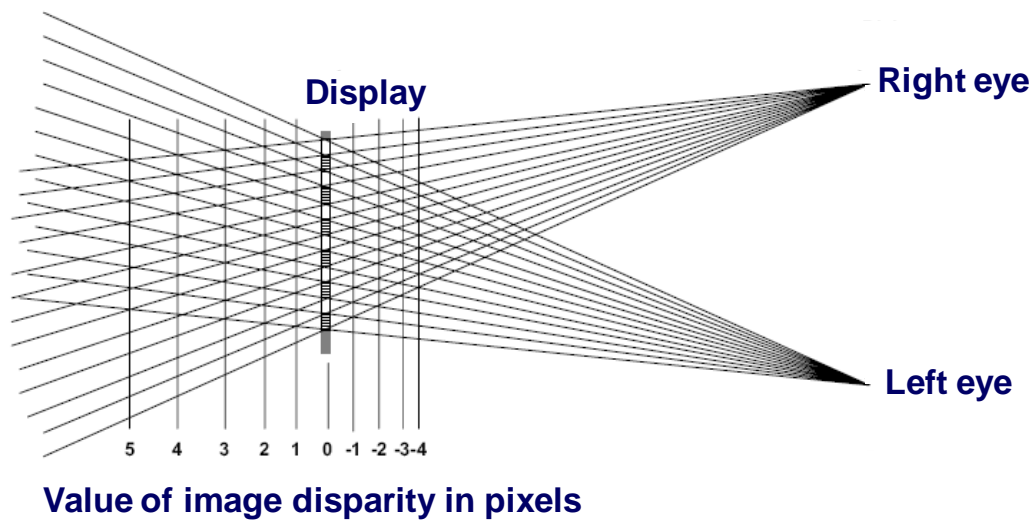


Fig. 2-6 Diagram of voxel and perceived depth[6].



Pixel disparity ↑, Perceived depth ↑, Number of voxels ↓

Fig. 2-7 Relation between pixel disparity, perceived depth, and number of voxels [6].

2.1.4 Light Efficiency

A display is composed of several components, such as a polarizer and a color filter. However, lights from a backlight are partly absorbed while passing through each component, as shown in Fig. 2-8. Therefore, image brightness is much lower than backlight brightness.

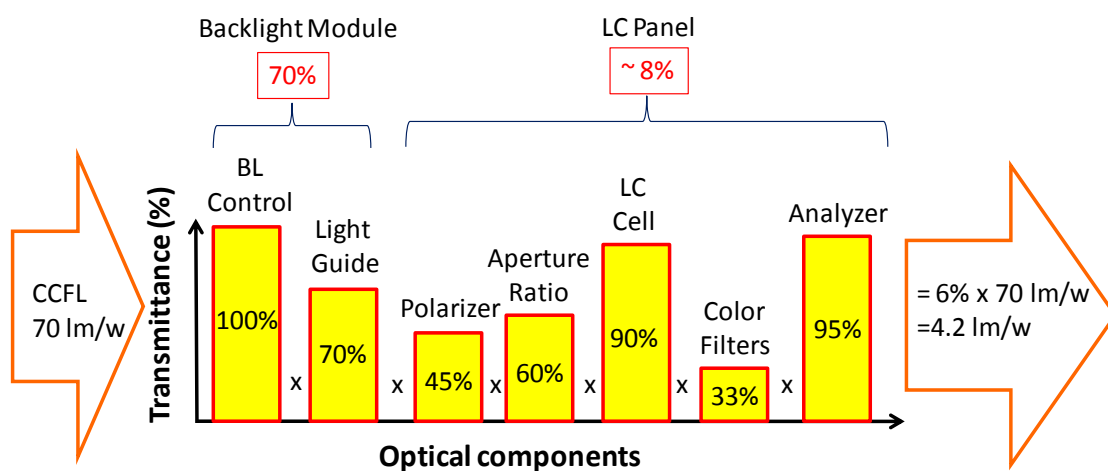


Fig. 2-8 Transmittance of each element in LCD [7].

A display producing high light efficiency presents bright images for a fixed power consumption LCD. Because 3D displays have more elements than 2D displays, maintaining light efficiency to present acceptable image brightness is essential for 3D displays.

2.1.5 Image Uniformity

Currently, backlights using LEDs are popular due to low power and local dimming technology. High directional LEDs are also utilized in side-emitted small 3D displays. However, in side-emission large 3D displays, a pixel distant from LEDs is less bright. So the image uniformity defined in the following equation is low [8].

$$\text{Image uniformity} \equiv \frac{\text{Minimum luminance (1~13)}}{\text{Average luminance (1~9)}} \times 100\% \quad (2 - 1)$$

The measuring points of a backlight are shown in Fig. 2-9. The tolerant image uniformity for humans is above 80%. Therefore, in designing 3D displays, direct-emission backlights are preferred to side-emission backlights for directing lights into different views and maintaining image uniformity.

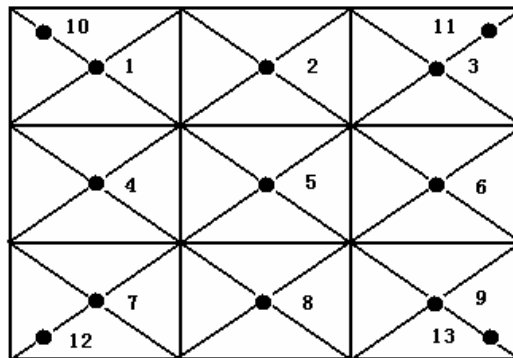


Fig. 2-9 Measuring points for image uniformity.

2.2 Stereoscopic Displays

Stereoscopic displays include shutter eyeglasses 3D displays and polarized

eyeglasses 3D displays. Shutter eyeglasses 3D displays contain a 120Hz LCD, a detector, and shutter eyeglasses [9]. The LCD shows left and right images sequentially at 120 Hz and the shutter eyeglasses switches on and off correspondingly. So the left and right eye receives different 2D images sequentially and the observer perceives stereoscopic effects, as shown in Fig. 2-10.

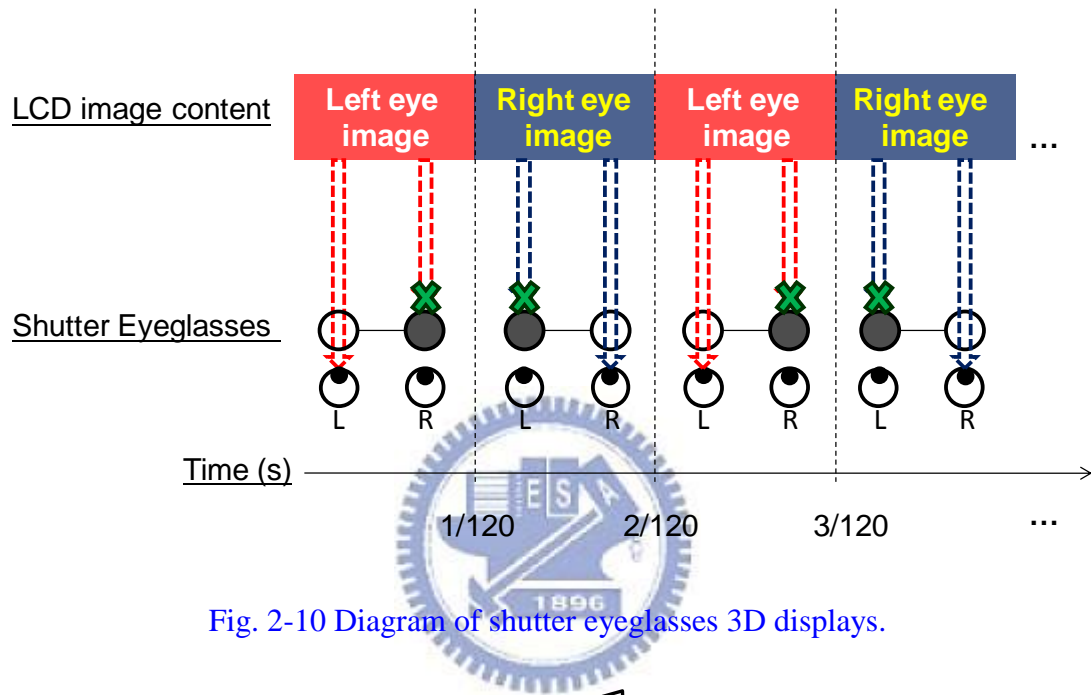


Fig. 2-10 Diagram of shutter eyeglasses 3D displays.

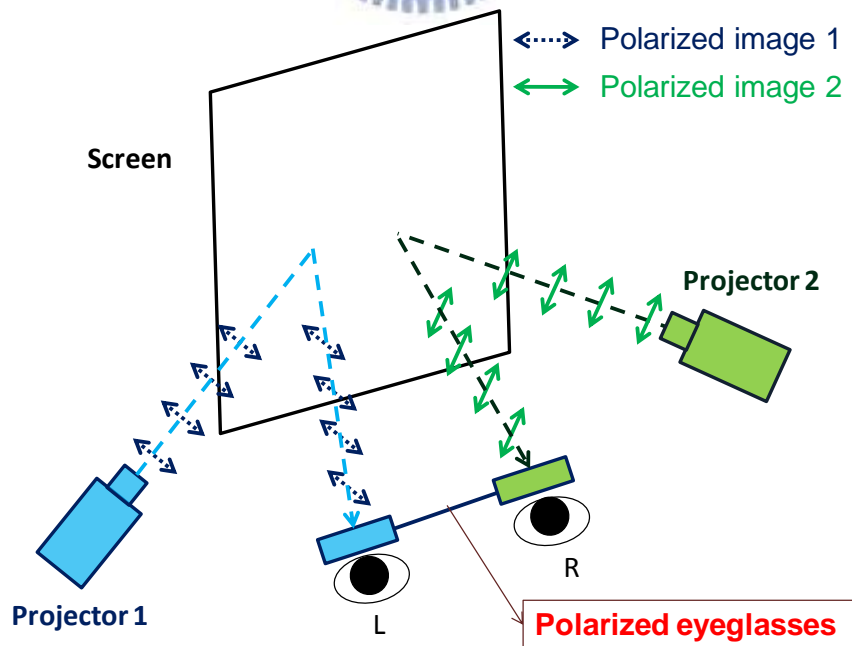


Fig. 2-11 Diagram of polarized eyeglasses 3D displays.

Polarized eyeglasses 3D displays include two projectors, a scattered screen, and polarized eyeglasses [10]. Two projectors produce different polarized 2D images and the screen scatters images. By wearing polarized eyeglasses, the left and right eye receives different polarized 2D images and the observer perceives stereoscopic effects, as shown in Fig. 2-11. Both of shutter and polarized eyeglasses 3D displays are widely used in movie theaters because several observers can see 3D movies simultaneously. However, the observer need to wear eyeglasses to perceive 3D images from stereoscopic displays. The motion parallax phenomenon is also a drawback because observers at different positions still see the same 3D image.

2.3 Auto-Stereoscopic Displays

Although stereoscopic displays have been widely utilized, because wearing eyeglasses is not required, multi-view and ease of fabrication, auto-stereoscopic displays are preferred to introduce 3D techniques into daily life. Since Holographic 3D displays have color distortion and large recording data requirements in 3D movies, several popular 2D-multiplexed 3D displays are introduced in the following.

2.3.1 Spatial-Multiplexed 3D Displays

2D-multiplexed 3D displays produce two different 2D images to the left and right eye separately. Then the brain combines two 2D images to introduce stereoscopic effects. The first 2D-multiplexed 3D displays are spatial-multiplexed 3D displays. As shown in Fig. 2-12, lights from different pixels are directed to corresponding views by using a parallax barrier or a cylindrical lens. The design equations of multi-view parallax barrier and multi-view cylindrical lens are shown in Fig. 2-13 and Fig. 2-14 [11] [12] [13] [14]. However, spatial-multiplexed multi-view 3D displays presented

low resolution 3D images because the 2D resolution per view was low due to divided pixels, as mentioned in Sec. 2.1.3. Parallax barrier 3D displays also produced low light efficiency since black areas blocked rays from backlights.

• Parallax barrier 3D display • Cylindrical lens 3D display

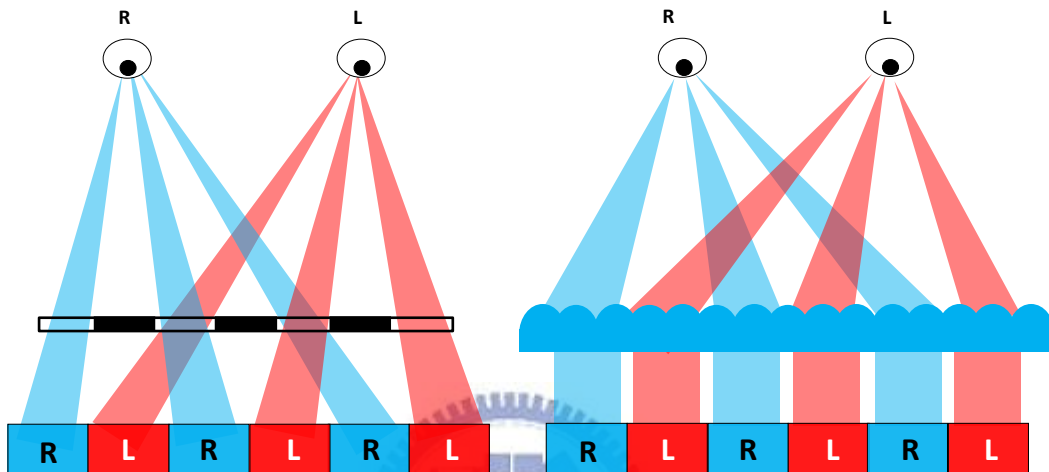


Fig. 2-12 Spatial-multiplexed 3D displays

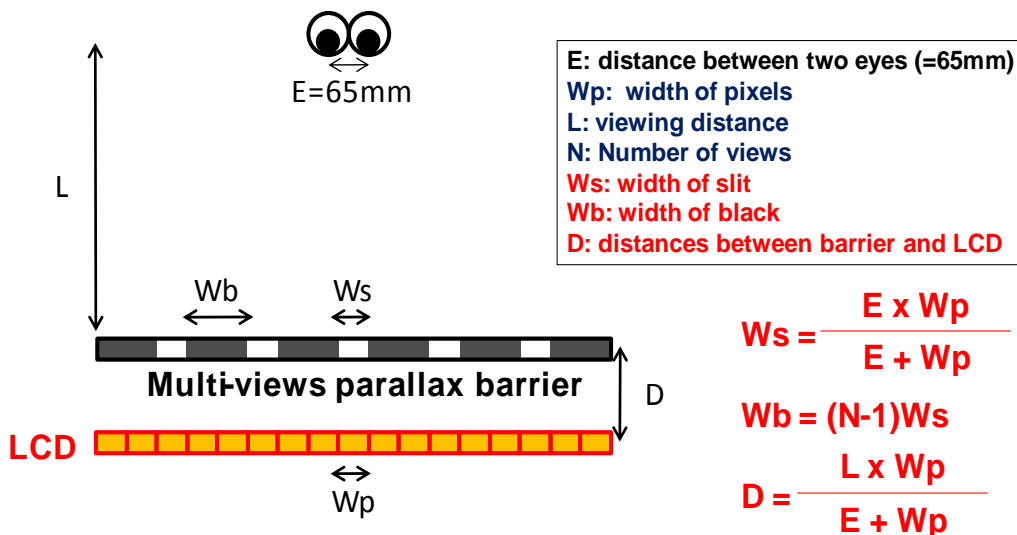


Fig. 2-13 Design equations of multi-view parallax barrier.

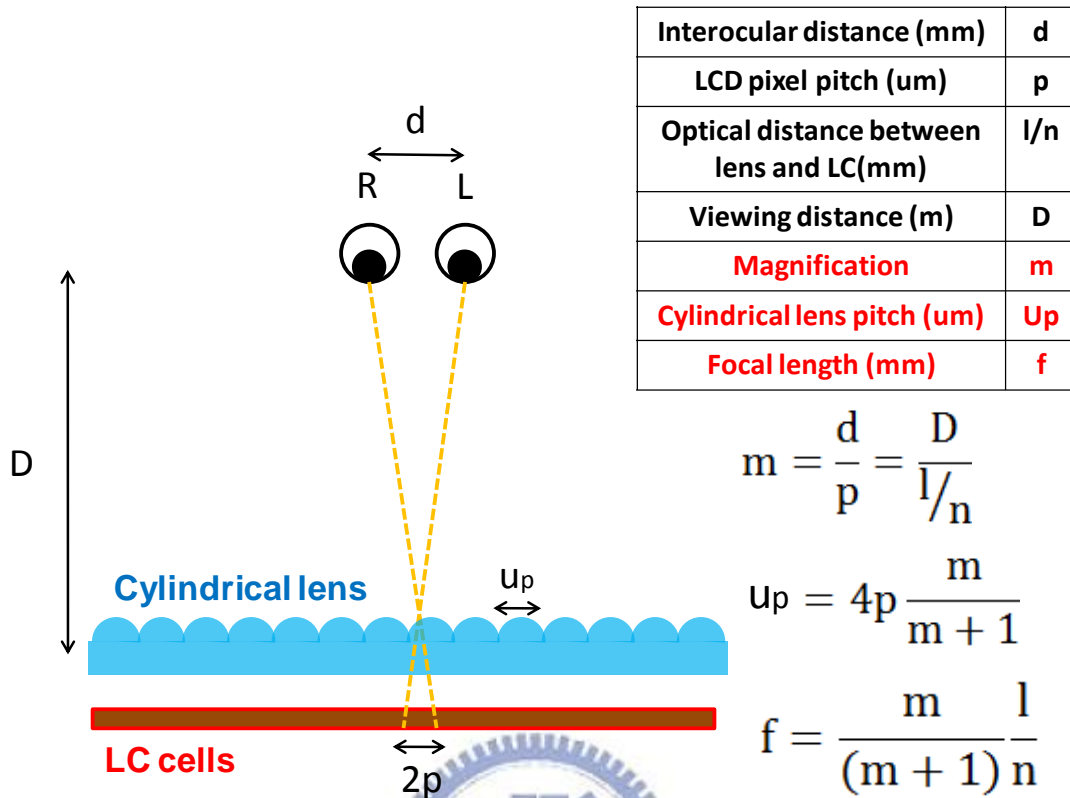


Fig. 2-14 Design equations of multi-view cylindrical lens.

2.3.2 Temporal-multiplexed 3D Displays

Temporal-multiplexed 3D displays were developed to solve low resolution and low light efficiency in spatial-multiplexed 3D displays. In Fig. 2-15 (a), a 3D mobile display based on sequentially switching backlight and focusing foil is proposed [15] [16] [17]. The crosstalk was less than 6% and image uniformity was higher than 80%. Another temporal-multiplexed 3D display is developed in Fig. 2-15 (b), including a side-emission sequential LED backlight, a 120Hz LCD, a directional light guide and a micro structure [18] [19] [20] [21]. Both the 3D displays presented full resolution and high brightness 3D images. However, the 120Hz side-emission backlight presented only two views and non-uniform images in large panels. Therefore, the two temporal-multiplexed 3D displays were only utilized in mobile applications.

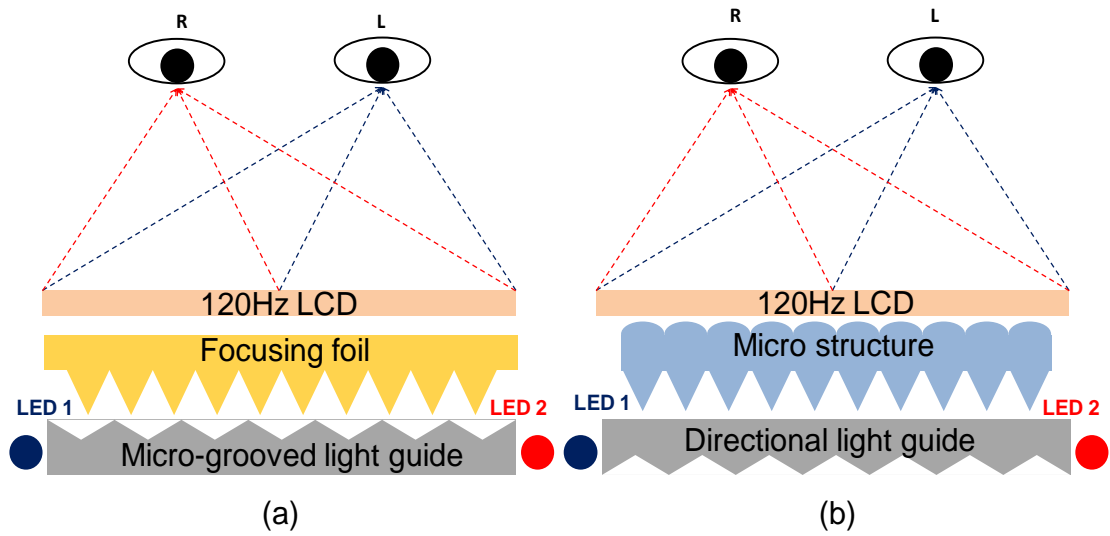


Fig. 2-15 Side-emission sequential backlight 3D displays.

2.3.3 Spatial-Temporal hybrid 3D Displays

Because spatial-multiplexed 3D displays produce low resolution 3D images and temporal-multiplexed 3D displays were only usable in mobile application, a spatial-temporal-hybrid 3D display using a time division LC parallax barrier and an AMOLED panel is shown in Fig. 2-16 [22].

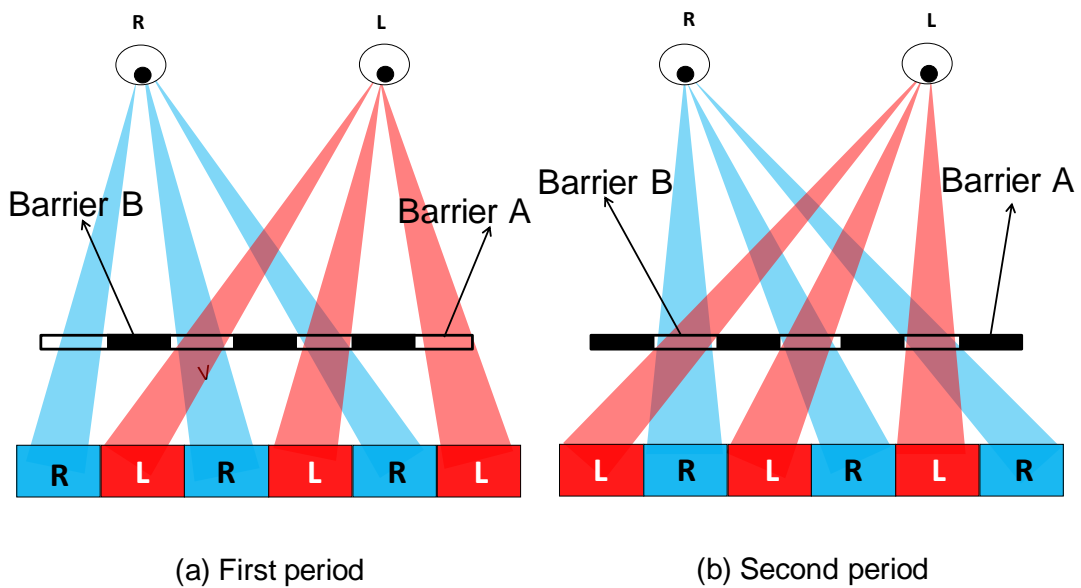


Fig. 2-16 Time division parallax barrier high resolution auto-stereoscopic display.

By controlling the OCB parallax barrier synchronizing the panel in different periods, the observer can perceive full resolution 3D images. Because the backlight was direct-emission, the spatial-temporal-hybrid 3D display was usable in large LCDs. The response time of Optical Controlled Birefringence (OCB) mode parallax barrier was about 5ms and the frame rate in the QVGA AMOLED panel was 240frame/sec. The number of views was two. However, the LC response time still limited number of views and the parallax barrier also produced low light efficiency.

2.4 Summary

Currently, stereoscopic displays have been widely utilized in movies. But wearing eyeglasses and the motion parallax phenomenon are drawbacks. Therefore, auto-stereoscopic displays were developed to introduce 3D techniques into daily life, including spatial-multiplexed 3D displays, temporal-multiplexed 3D displays, and spatial-temporal hybrid 3D displays. However, image resolution, light efficiency, number of views and image uniformity in large panels are still drawbacks in existing 3D displays. One solution for proposing auto-stereoscopic displays is designing 3D backlights because backlights are the greatest difference between 2D displays and 3D displays, as shown in Fig. 2-17.

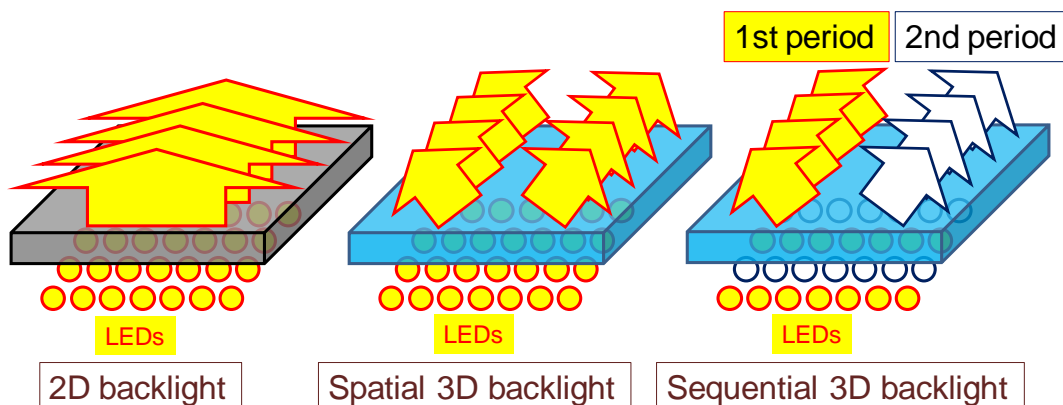


Fig. 2-17 2D backlight and 3D backlights.

In 2D displays, backlights produce uniform and bright lights. However, in 3D displays, backlights are not only light sources, but also light guides to produce viewing-zones spatially or sequentially. Therefore, by combining techniques from the spatial-multiplexed 3D displays and the temporal-multiplexed 3D displays mentioned above, a spatial-temporal hybrid multi-view 3D display was proposed. Considering average crosstalk, viewing-zone uniformity, resolution, light efficiency, number of views and image uniformity in large LCDs, designing processes of the proposed auto-stereoscopic display were analyzed and discussed.



Chapter 3

Spatial-Temporal Hybrid 3D Display

A spatial-temporal hybrid multi-view 3D display was proposed to solve drawbacks in existing auto-stereoscopic displays, including resolution, light efficiency, number of views, and image uniformity in large LCDs. The proposed 3D display includes a four-directional temporal backlight, a 240 Hz LCD and a multi-view parallax barrier, as shown in Fig. 3-1. The four-directional temporal backlight produced four viewing zones sequentially. Then the multi-view parallax barrier divided each viewing zone to produce multi-view 3D images. The design of each element is introduced in this chapter.

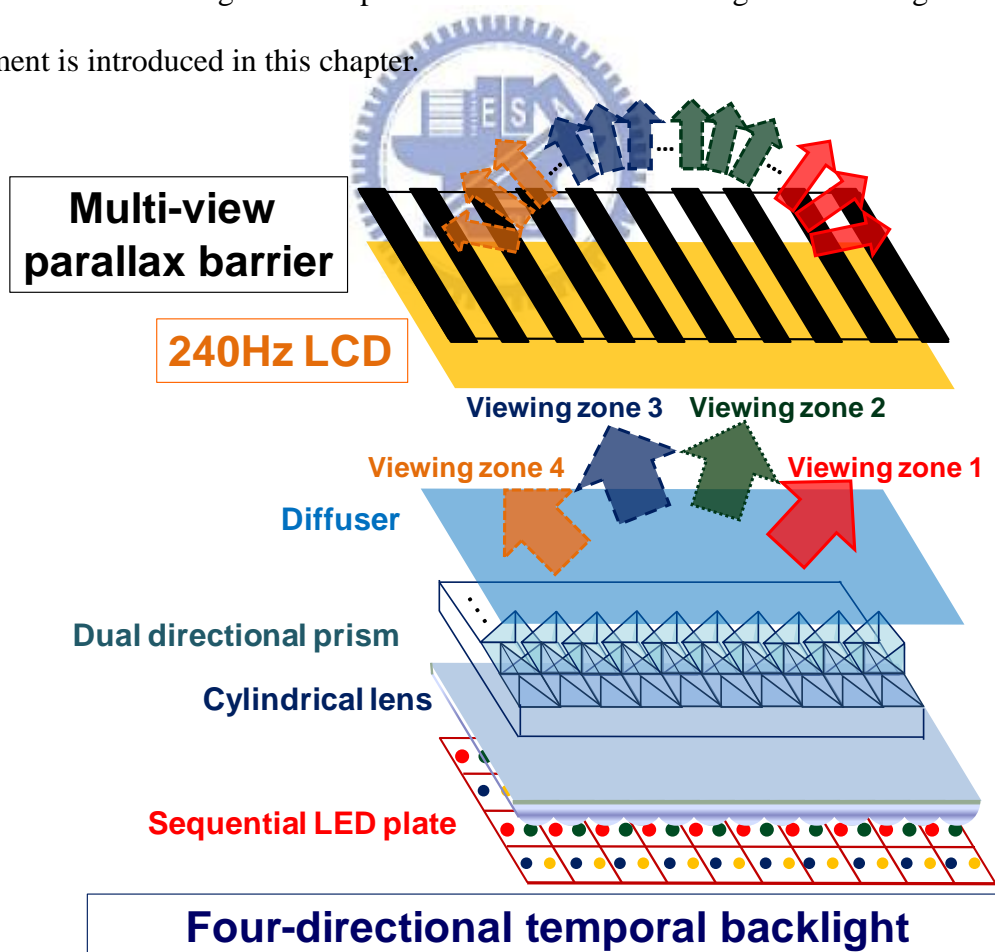


Fig. 3-1 Structure of spatial-temporal hybrid multi-view 3D display.

3.1 Four-Directional Temporal Backlight

As mentioned in Sec 2.4, backlight systems are the greatest difference between 2D displays and 3D displays. Therefore, developing a 3D backlight makes the 3D display design possible. Considering the light source direction, direct-emission backlights are preferred to side-emission backlights to present a uniform image on large LCDs. Considering the backlight state, sequential backlights are better than full on backlights in creating high resolution 3D images. Consequently, a four-directional temporal backlight is shown in Fig. 3-2, including a sequential LED plate, a cylindrical lens, a dual directional prism, and a diffuser. Following, the function of each element is introduced.

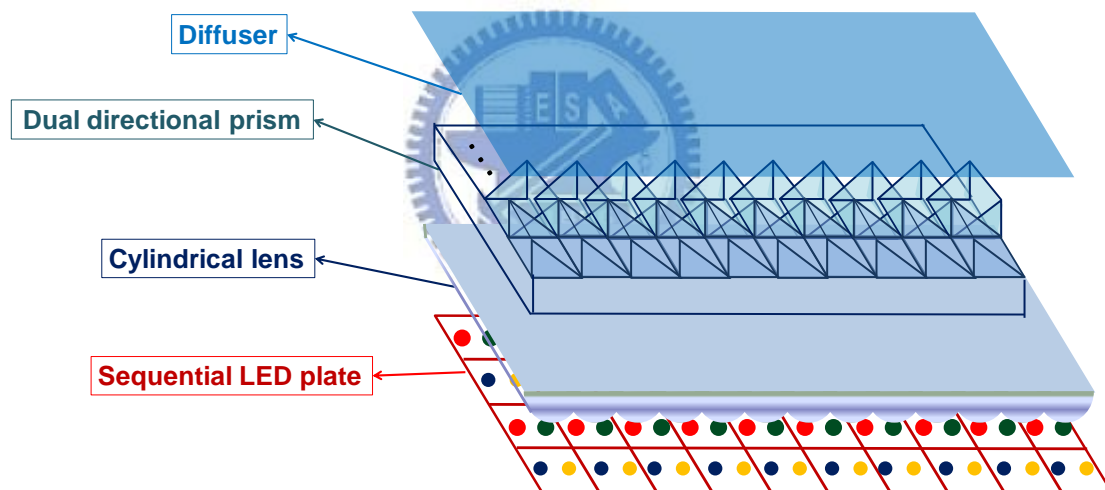


Fig. 3-2 Four-directional temporal backlight.

3.1.1 Sequential LED Plate

Cold cathode fluorescent lamps (CCFL) were widely used in display technologies. However, because improved power saving, longer lifetime, mercury issues and local dimming technology, light-emitting diodes (LED) replaced CCFL. Utilizing the local dimming technology, a sequential LED plate in the four-directional

temporal backlight is shown in Fig. 3-3. All LEDs in the backlight are white LEDs developed by stimulating blue LEDs to yttrium aluminum garnet (YAG). To prevent from flicker, four white LEDs switch on and off sequentially at 240Hz. As mentioned in Sec 2.3.1, a sequential LED plate not only improves image resolution, but also increases light efficiency in backlight systems.

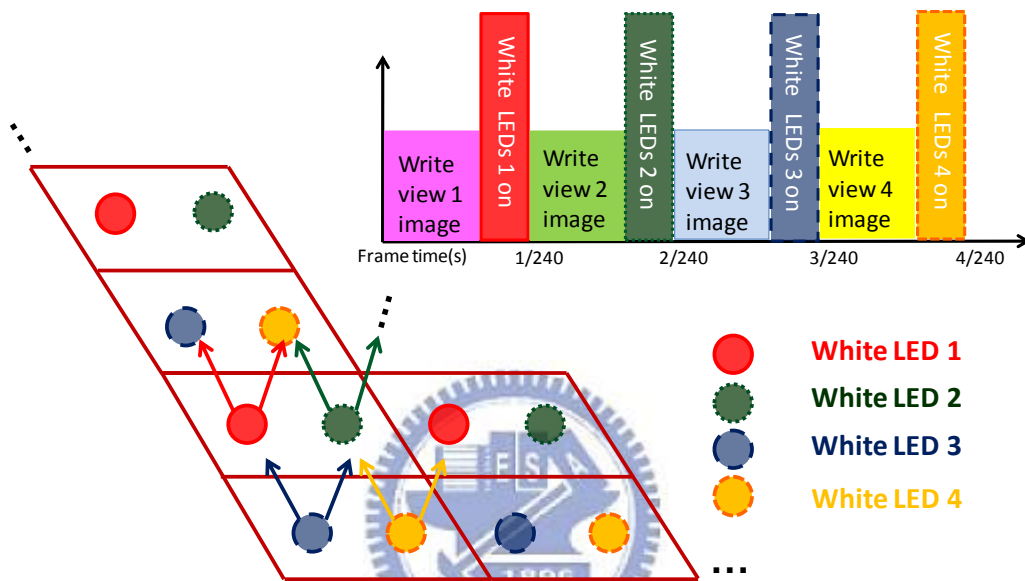


Fig. 3-3 240Hz sequential LED plate.

3.1.2 Cylindrical Lens

At the EURO SID conference in 1996, Philips proposed a cylindrical lens 3D display in Fig. 2-14. By using geometric optics, a cylindrical lens was designed to direct rays to specific viewing directions. Cylindrical lens 3D displays are easy to fabricate and have higher light efficiency than parallax barrier 3D displays have. Therefore, in the four-directional temporal backlight, by adding a cylindrical lens above the sequential LED plate, rays from different colors of white LEDs are directed at two certain viewing angles, as shown in Fig. 3-4.

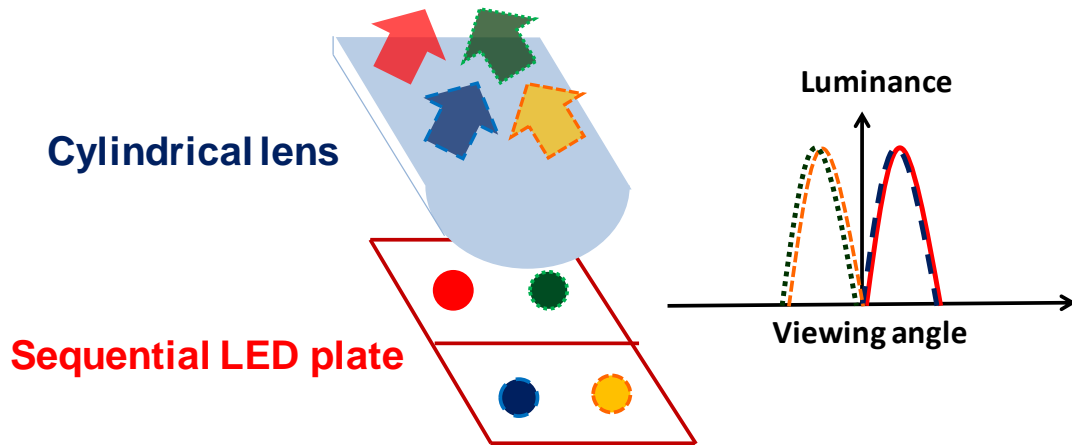


Fig. 3-4 Diagram of cylindrical lens.

3.1.3 Dual Directional Prism

After adding a cylindrical lens, two viewing zones were formed. However, as mentioned in Sec 3.1.1, the proposed display produced four viewing zones synchronizing four sequential white LEDs. So a dual directional prism must be added above the cylindrical lens. As shown in Fig. 3-5, in first step, the whole panel is divided into even rows and odd rows. Next, using refraction theory, by adding a micro prism 1 on even rows, light distributions of even rows shift to the right. Similarly, when a micro prism 2 is added on odd rows, light distributions shift to the left. Finally, by combining micro prism 1 and micro prism 2, a dual directional prism was fabricated to increase viewing zones from two to four. Therefore, the proposed 3D display produced four viewing zones corresponding to the sequential LED backlight.

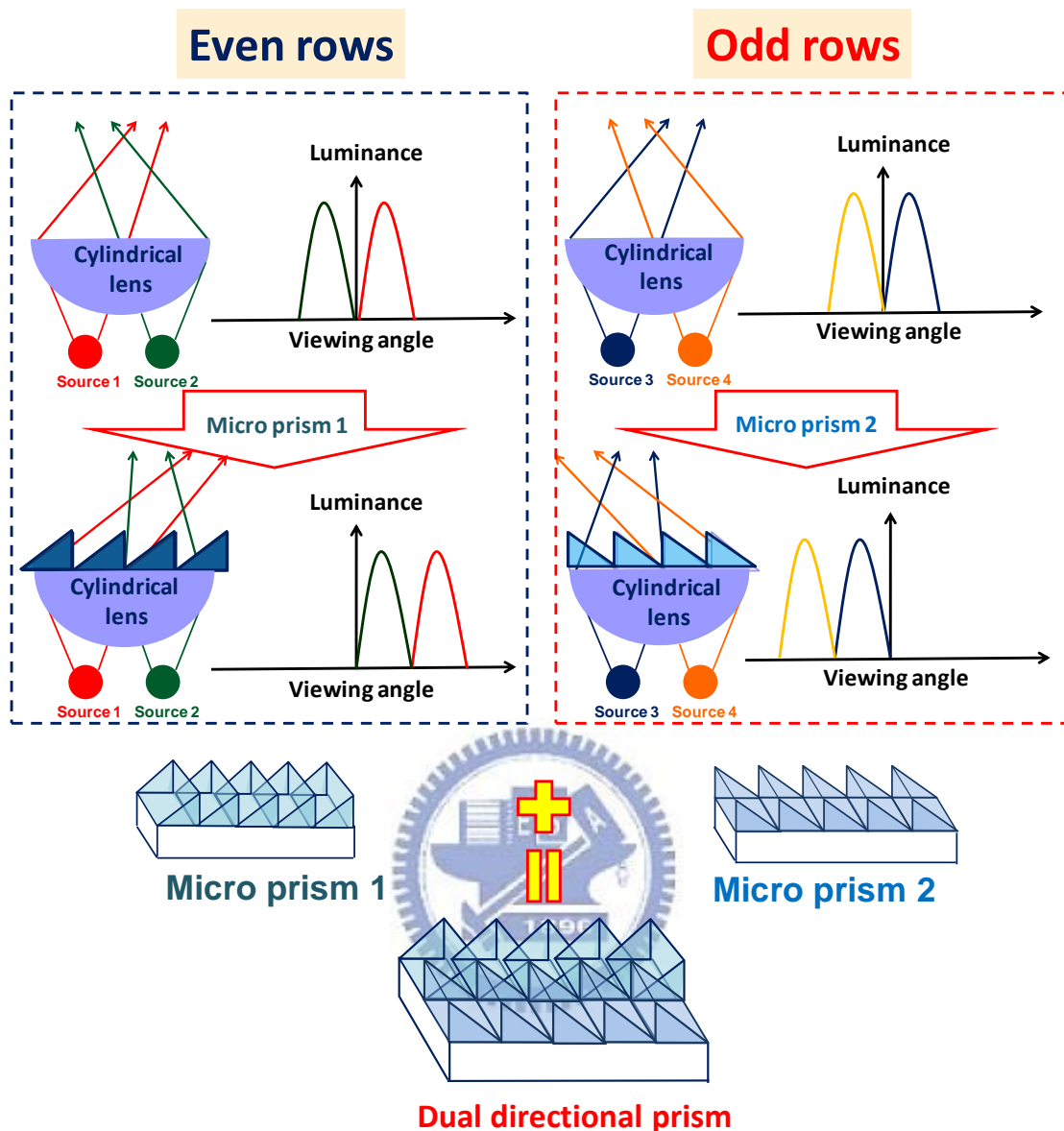


Fig. 3-5 Diagram of dual directional prism.

3.1.4 Diffuser

A diffuser is an optical film that can scatter lights from a backlight to improve image uniformity. Currently, most diffusers are particle-diffusing diffusers by coating micro-sized beads with binding resin on a substrate, as shown in Fig. 3-6.

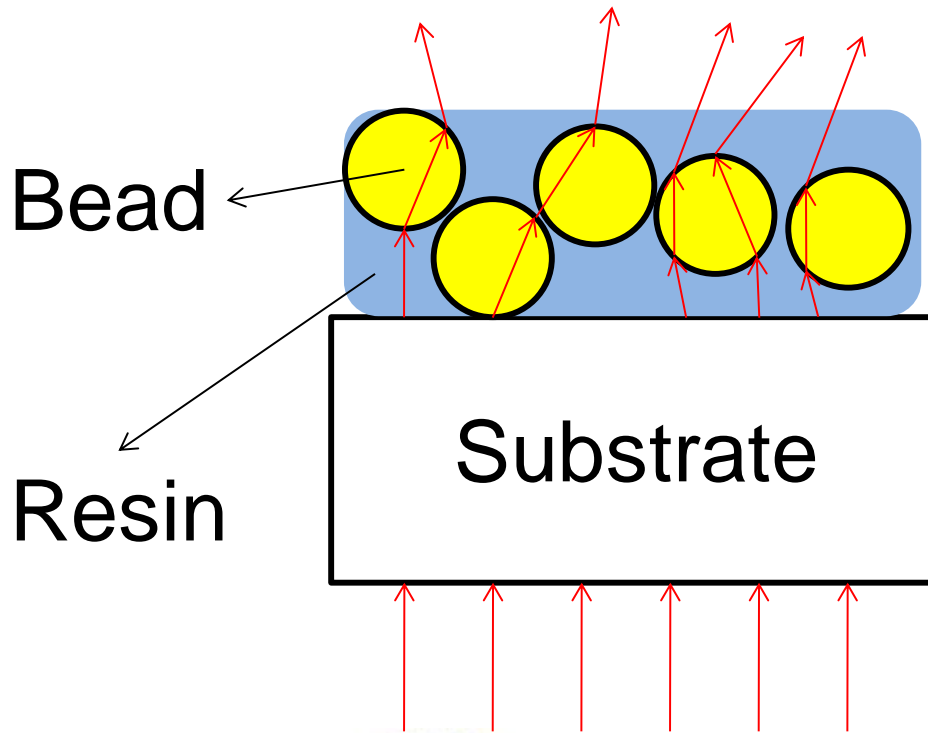


Fig. 3-6 Diagram of diffusers.

The light transmittance value and the haze value are important optical criteria. Light transmittance affects image brightness and haze affects viewing-zone uniformity and image uniformity [23]. Equations for calculating transmittance and haze are shown in Fig. 3-7. A diffuser with strong optical performance has a high light transmittance value and a high haze value. The haze value is defined as the scattered light measured divided by the total transmitted light measured in an Integrating Sphere. For example, in Fig. 3-7, a diffuser with a haze value of 80% means that 20% incident light is observed in $\pm 5^\circ$ range in a diffuser spectrum. So a diffuser with a high haze value has uniform light distribution and uniform images. Consequently, in the four-directional temporal backlight, by adding an adequate diffuser in front of the dual directional prism, the viewing-zone uniformity was increased and observers perceived continuous and uniform 3D images.

T: Transmittance H: Haze l: Coating thickness d: Particle diameter B: Beads weight R: Resin weight	$T = 127.36 \left(\frac{l}{d}\right)^{-0.345} \left(\frac{B}{R}\right)^{-0.245}$ $H = 92.6 - 46.33e^{-1.77\left(\frac{l}{d}\right)}, B/R=8/2$ $H = 92.6 - 10.24e^{-0.82\left(\frac{l}{d}\right)}, B/R=7/3$ $H = 92.6 - 6.76e^{-0.66\left(\frac{l}{d}\right)}, B/R=6/4$
---	--

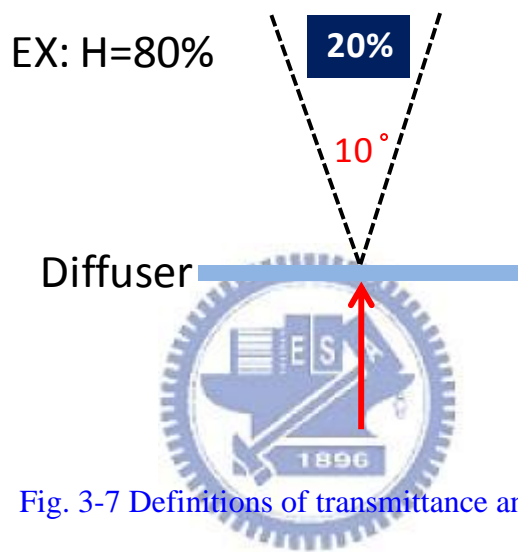


Fig. 3-7 Definitions of transmittance and haze.

3.2 240Hz LCD

Most displays include a backlight system and a LCD. In the spatial-temporal hybrid 3D display, as mentioned in Sec 3.1, the four-directional temporal backlight gave four viewing zones sequentially at 240Hz to prevent flicker. Therefore, a LCD in the spatial-temporal hybrid multi-view 3D display displays images at 240 Hz, sequentially synchronizing the temporal backlight, as shown in Fig. 3-8.

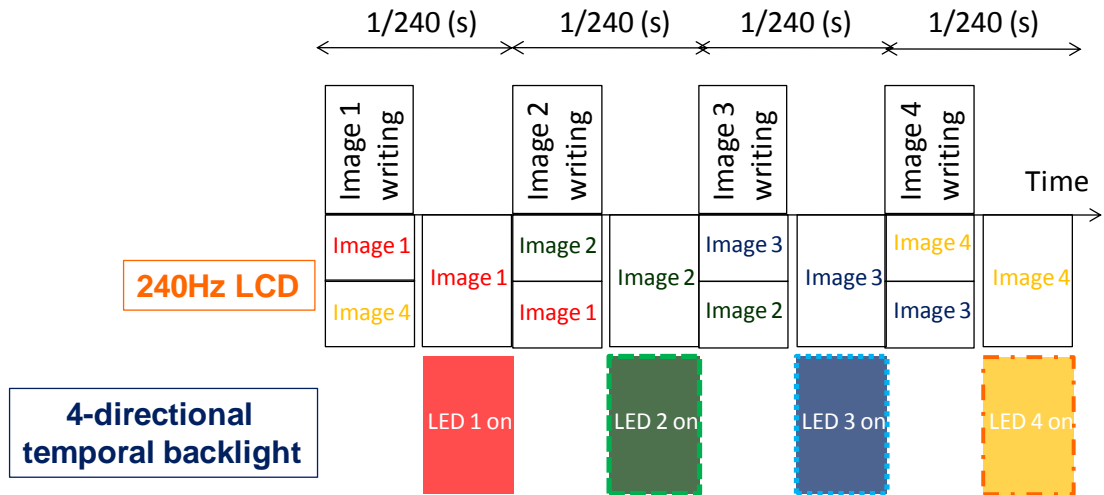


Fig. 3-8 Diagram of four-directional temporal backlight and 240Hz LCD.

3.3 Multi-View Parallax Barrier

After designing the four-directional temporal backlight and the 240Hz LCD, the temporal 3D display produced four viewing zones sequentially.

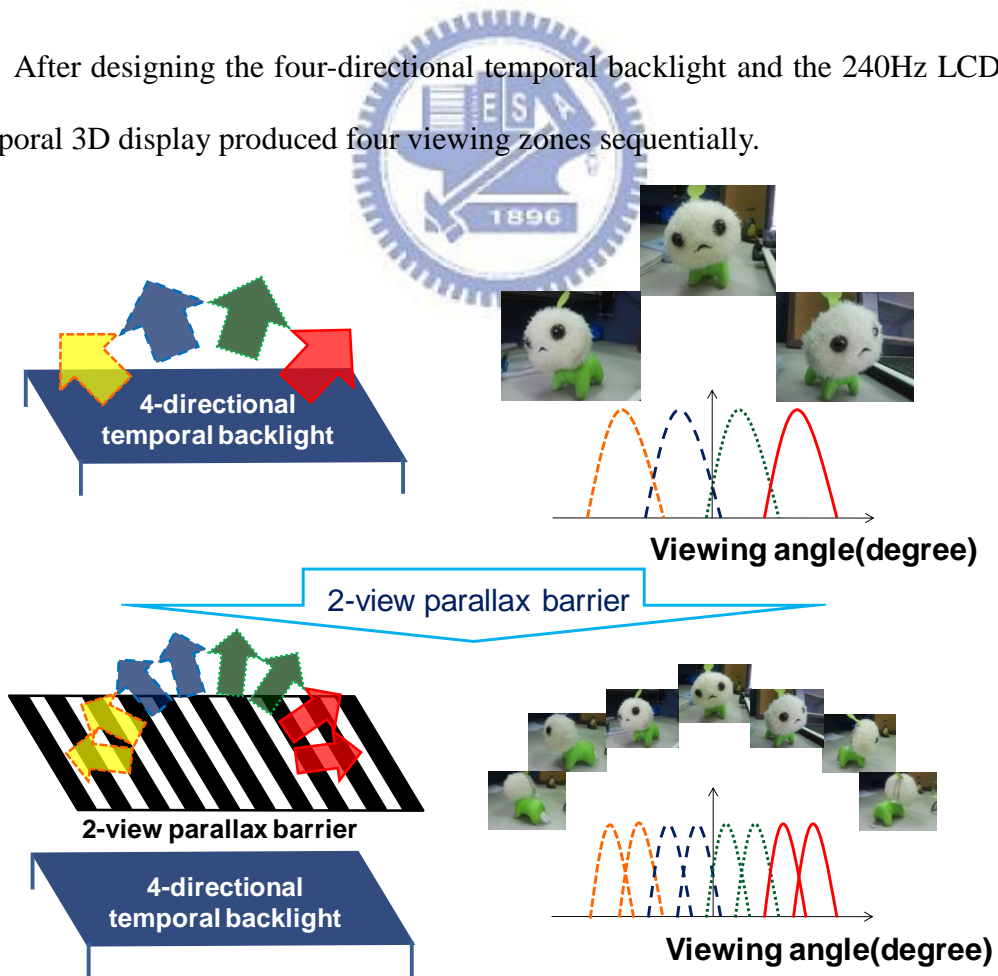


Fig. 3-9 Multi-views parallax barrier diagram.

Referring to spatial-multiplexed 3D displays in Sec. 2.3.1, when a multi-view parallax barrier is added, number of views increases and an observer perceives different 3D images while moving to different positions. For example, by adding a front 2-view parallax barrier, each viewing zone from the four-directional temporal backlight is divided into two views. So the number of views is increased from four to eight, and 3D images are increased from three to seven, as shown in Fig. 3-9.

3.4 Summary

In the spatial-temporal hybrid multi-view 3D display, the four-directional temporal backlight is the key to solve drawbacks in existing auto-stereoscopic displays, including resolution, light efficiency, number of views, and image uniformity in large LCDs.

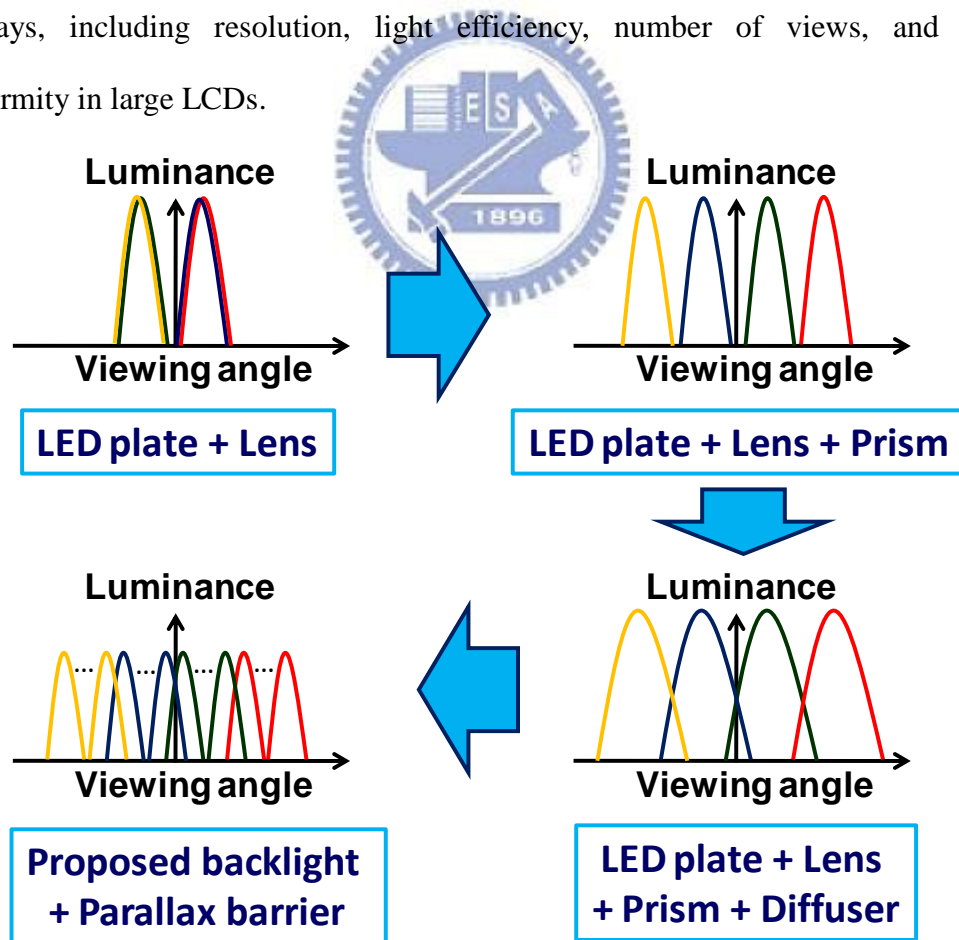
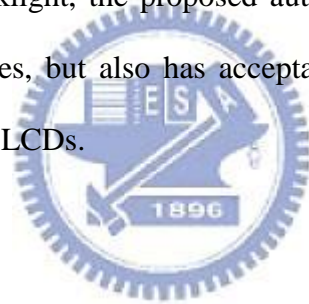


Fig. 3-10 Light distribution of spatial-temporal hybrid multi-view 3D display.

The light distribution of spatial-temporal hybrid multi-view 3D display is shown in Fig. 3-10. The first element in the backlight is a sequential LED plate, which is comprised of four white LEDs switching on and off sequentially at 240Hz. By adding a cylindrical lens, lights from the LED plate are directed into two specific viewing zones. Then, using a dual directional prism, viewing zones are increased from two to four synchronizing the four sequential white LEDs. Finally, by adding a diffuser on the dual directional prism, lights from backlight are scattered to improve viewing-zone uniformity and eliminate edges. Consequently, the four-directional temporal backlight produces four uniform viewing zones separately and sequentially. Finally, by using a 240 Hz LCD and a multi-view parallax barrier above the four-directional temporal backlight, the proposed auto-stereoscopic display not only presents multi-view 3D images, but also has acceptable resolution, light efficiency, and image uniformity in large LCDs.



Chapter 4

Simulations for Proposed 3D Backlight

This chapter evaluates the proposed 3D backlight by using Geometric Optics. Then the four-directional temporal backlight was also optimized for low average crosstalk and high viewing-zone uniformity defined in Sec. 2.1.

4.1 Geometric Optics Evaluation of Proposed 3D Backlight

The four-directional temporal backlight produced four viewing zones sequentially by using a 240Hz sequential LED plate, a cylindrical lens and a dual directional prism. This section uses Geometric Optics to calculate the ideal direction of each viewing zone and verify the backlight design proposed in Sec. 3.1.

4.1.1 Refracted Procedure in Cylindrical lens

The pitch (P) and divergent angle (Θ) were parameters in the LED plate. The lens curvature radius (R) and distance from LEDs were parameters in the cylindrical lens. The first refraction phenomenon is lights illuminating from air to the cylindrical lens, as shown in Fig. 4-1. By using the thick lens formula, the incident angle from the lens to air (u_1) was obtained. Then, the second refraction phenomenon is lights illuminating from the cylindrical lens to air, as shown in Fig. 4-2. By using Snell's Law, the angle after the lens (u_2) was also calculated.

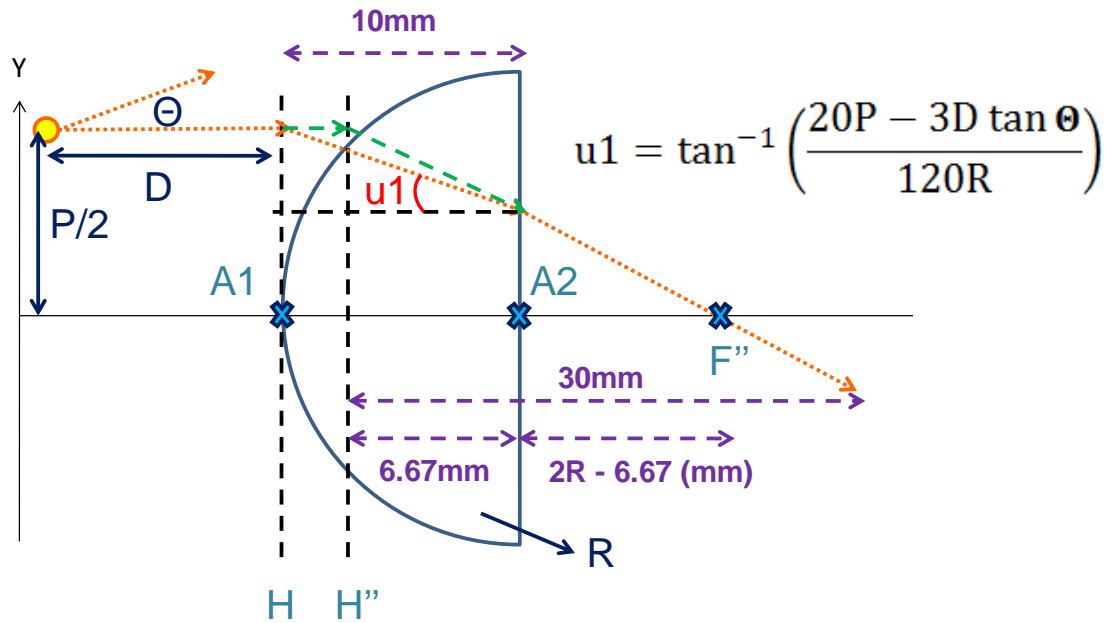


Fig. 4-1 Refraction from air to the cylindrical lens.

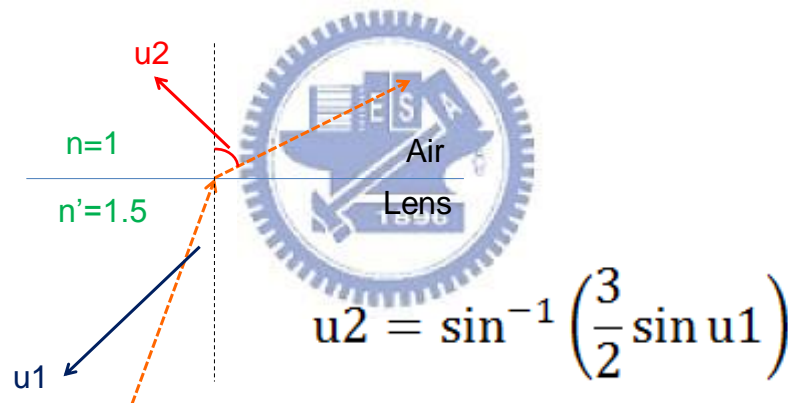


Fig. 4-2 Refraction from the cylindrical lens to air.

4.1.2 Refracted Procedure in Prism

The parameter simulated in the prism was the obtuse angle (A). For example, in micro prism 2, the first refraction phenomenon is lights illuminating from the air to the prism, as shown in Fig. 4-3. By using Snell's law and Geometrics, the incident angle from the prism to air (u_3) was obtained. Then, the second refraction phenomenon is lights illuminating from the prism to air, as shown in Fig. 4-4. By using Snell's law, the angle of each viewing zone (u_4) was obtained. Calculations in

the micro prism 1 were similar to the micro prism 2.

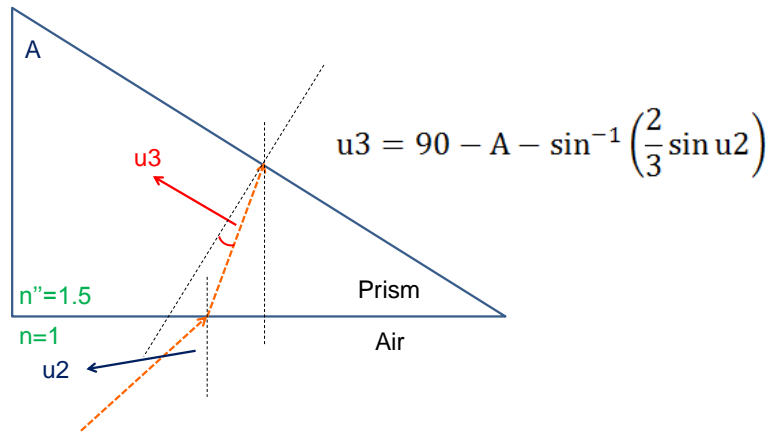


Fig. 4-3 Refraction from air to the prism.

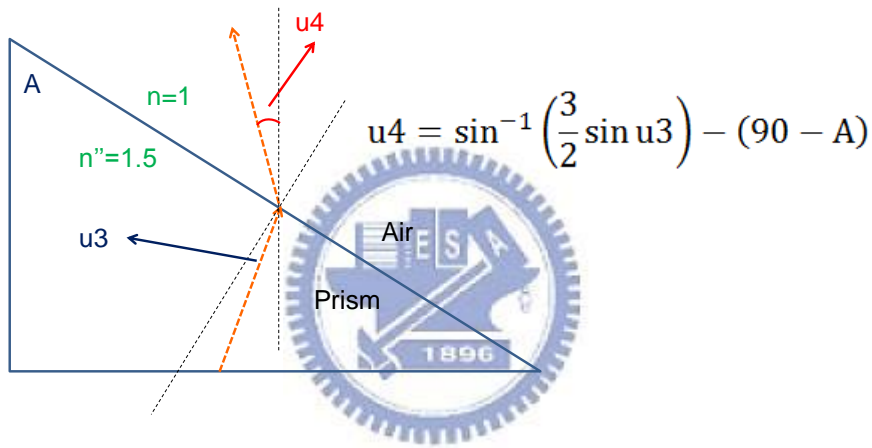


Fig. 4-4 Refraction from the prism to air.

By combing above equations together, in micro prism 2, the equation for calculating two viewing zones directions (u_4) was obtained as follow. Another two viewing zones produced by the micro prism 1 were similar to the two viewing zones produced by the micro prism 2. Therefore, the equation also verified that the proposed backlight produced four viewing zones corresponding to different LED locations (P).

$$u_4 = \sin^{-1} \left\{ \frac{3}{2} \cos \left[A + \tan^{-1} \left(\frac{20P - 3D \tan \theta}{120R} \right) \right] \right\} - 90 + A \quad (4-1)$$

4.2 Simulations of Four-Directional Temporal Backlight

After calculations by using Geometric Optics, this section discusses simulations and optimization by using optical software (LighTools 6.1.0), including a sequential LED plate, a cylindrical lens, a dual directional prism, and a diffuser. Finally, the proposed backlight was confirmed by comparing the calculation results and simulation results.

4.2.1 Sequential LED Plate

White LEDs in the backlight switched on and off at 240Hz to produce four viewing zones sequentially, as mentioned in Sec. 3.1.1. There are two parameters in the LED plate, as shown in Fig. 4-5. The first parameter was the distance between neighboring LEDs (P). LEDs fabricated in small package diameters have small P values. The distance between neighboring LEDs is as close as possible to eliminate hot spots phenomenon in Fig. 4-6.

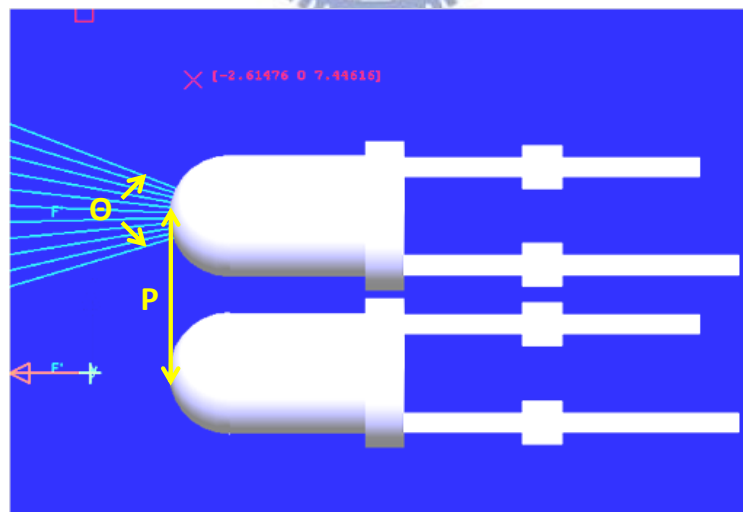


Fig. 4-5 Parameters of sequential LED plate.

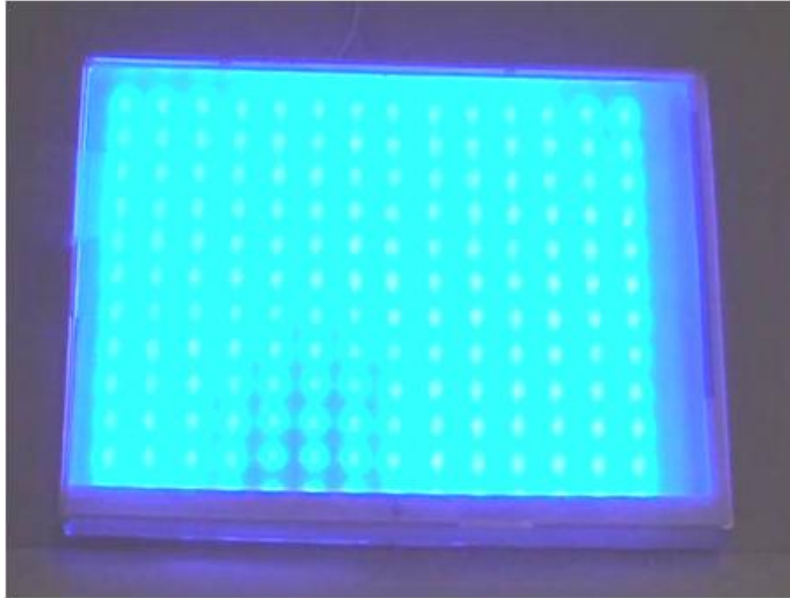


Fig. 4-6 Hot spots phenomenon.

The second parameter was the divergent angle of LEDs (Θ). As mentioned in Sec 2.4, because 3D backlights must have directional lights, the divergent angle of LEDs was as small as possible. Fig. 4-7 shows comparisons between white LEDs built using LighTools 6.1. The model No.312 had minimum P and Θ . Therefore, optimized white LEDs were: $(P, \Theta) = (4\text{mm}, \pm 20^\circ)$.

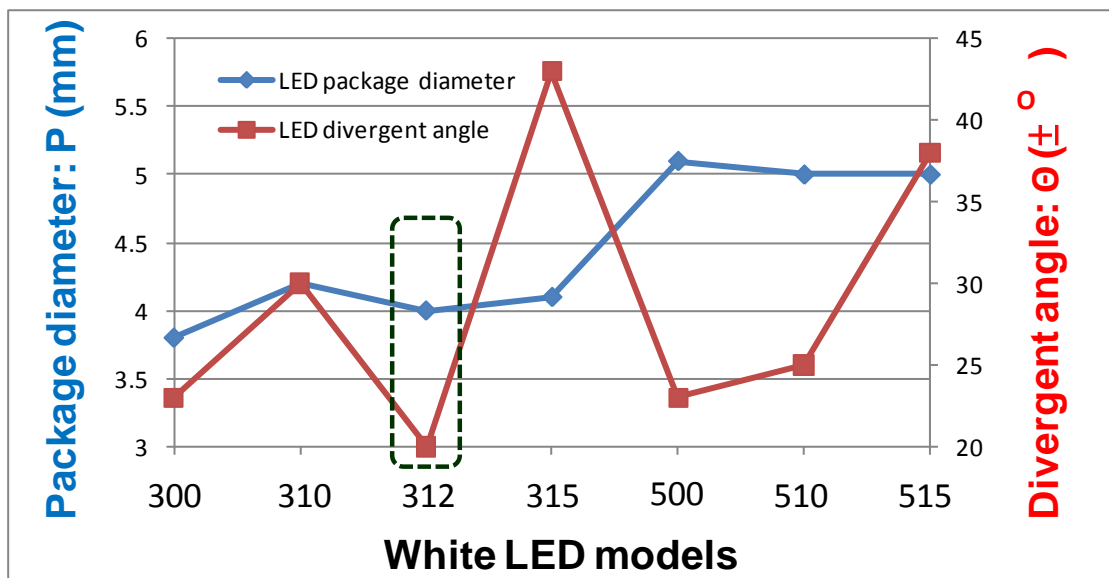


Fig. 4-7 Comparisons between white LEDs built using LighTools 6.1.

4.2.2 Cylindrical Lens

Above the sequential LED plate, a cylindrical lens directed lights in two specific directions. The light distribution occurred after the cylindrical lens was related to the focal length and the lens location. Therefore, the curvature radius (R) and the distance between the lens and LEDs (D) are two parameters in designing cylindrical lens, as shown in Fig. 4-8.

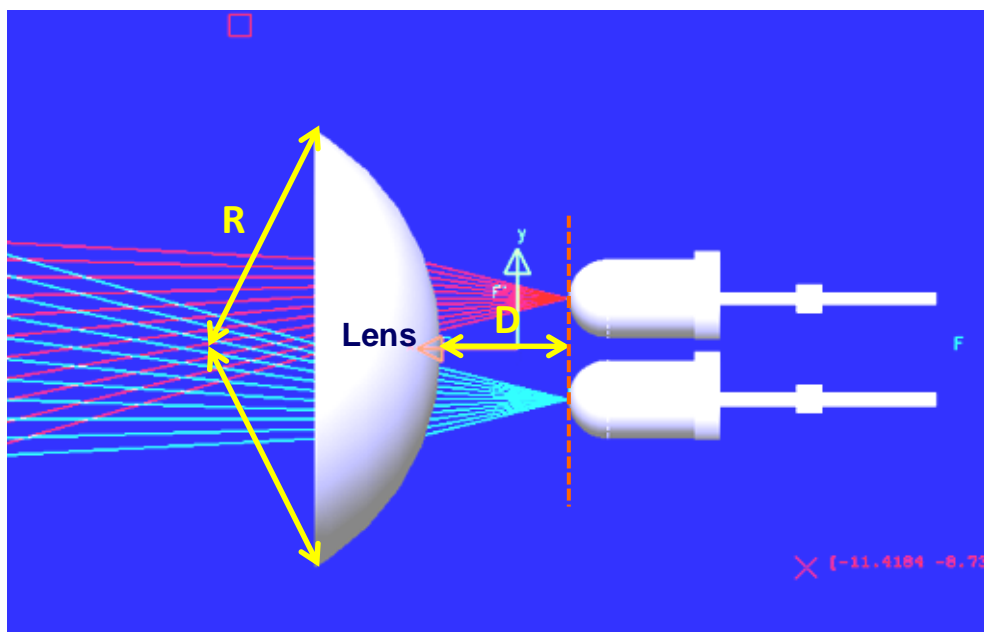


Fig. 4-8 Two parameters in cylindrical lens.

In the optimization process, R was decided first. Then by adjusting D , different light distributions were obtained. The example of $R=10\text{mm}$ is shown in Fig. 4-9. When $D=12\text{mm}$, angular differences between viewing zones were almost the same, so the crosstalk of each viewing zone was similar. Five optimized lens samples in different R values are shown Fig. 4-10. The sample with smallest R value had lowest average crosstalk. Because the lens thickness was 10mm , minimum of R was 10mm . Therefore, the optimized cylindrical lens was: $(R, D) = (10\text{mm}, 12\text{mm})$.

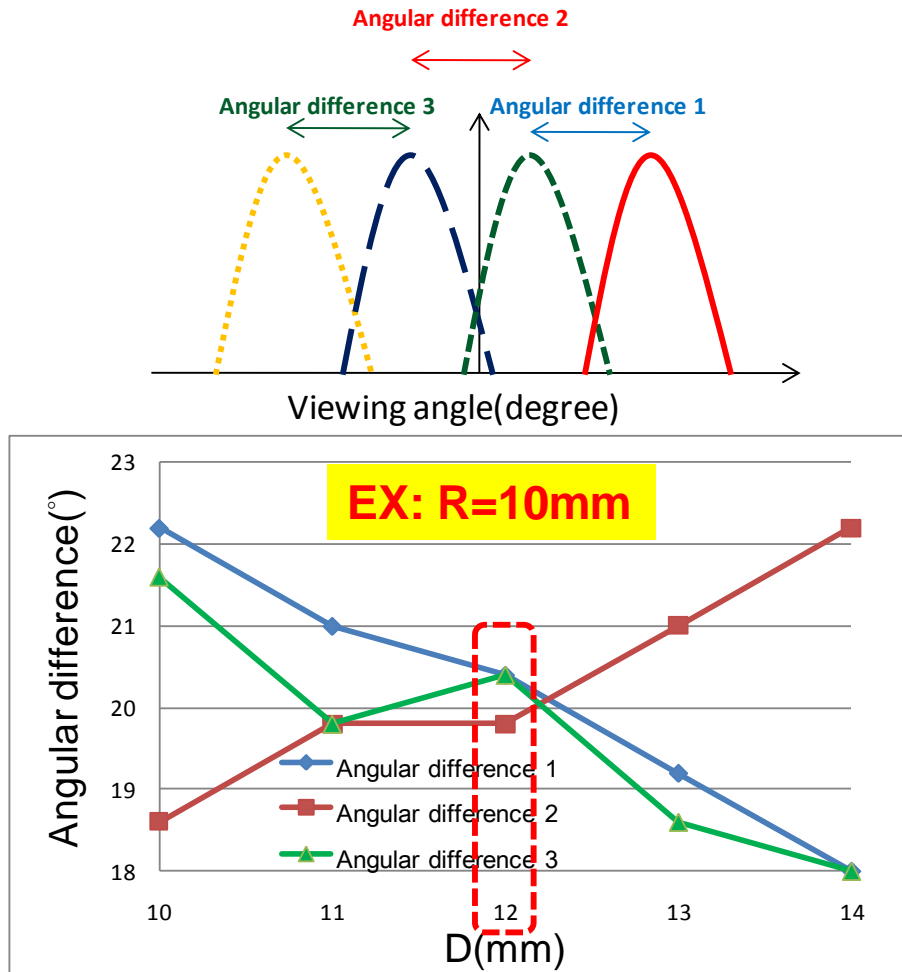


Fig. 4-9 Angular difference vs. Distance between lens and LEDs (D) as R=10mm.

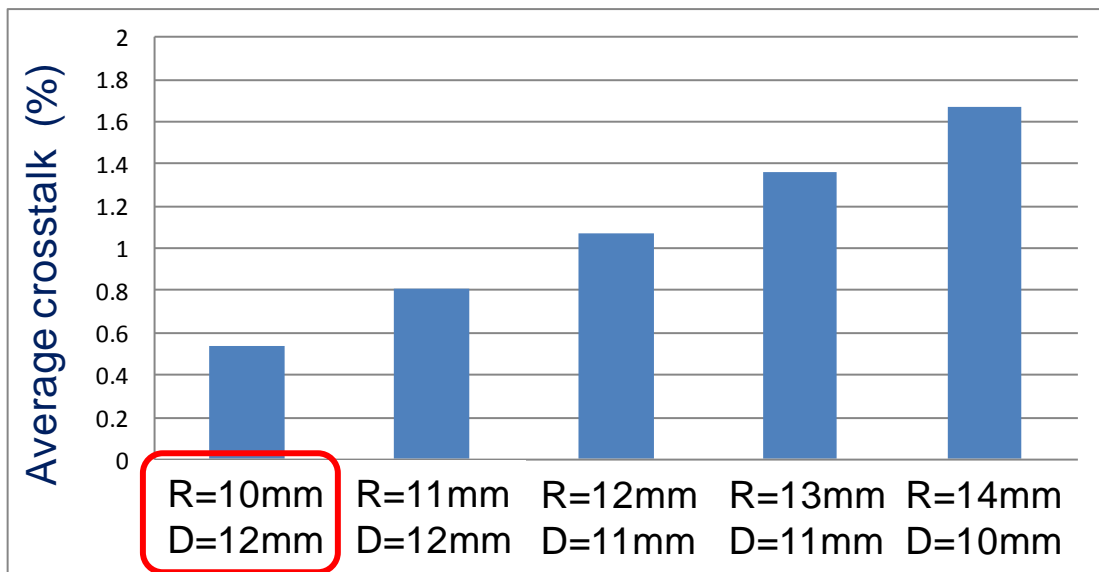


Fig. 4-10 Five cylindrical lens samples after optimization.

4.2.3 Dual Directional Prism

After adding a cylindrical lens, lights from LEDs illuminated two specific viewing angles. However, as mentioned in Sec. 3.1.1, the proposed 3D backlight produced four viewing zones corresponding to four sequential white LEDs. So a dual directional prism was added to increase viewing zones from two to four. As shown in Fig. 4-11, micro prism 1 and micro prism 2 have the same structure but lay in opposite directions. The length (L), height (H) and width (W) were 20 μ m, 12 μ m, 4mm. The obtuse angle (A) was 60°. The refraction index of the prism was nearly 1.5. As shown in Fig. 4-12, by using Snell's Law, micro prism 1 shifts light distributions on even rows to the right. Similarly, micro prism 2 shifts light distributions on odd rows to the left. The four viewing zone directions were 30°, 10°, -10°, and -30° in simulation. In calculation by using Eq. 4-1, the four viewing zone directions were 27°, 11°, -11°, and -27°. Consequently, the backlight produced four viewing zones separately by using the cylindrical lens and the dual directional prism.

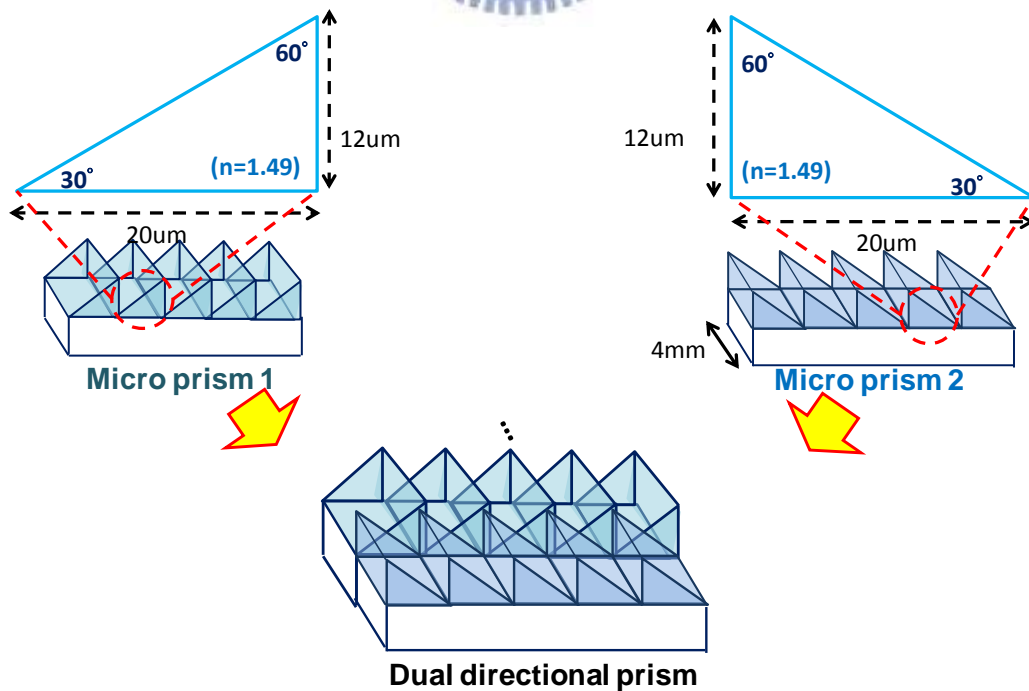


Fig. 4-11 Diagram and parameters of dual directional prism.

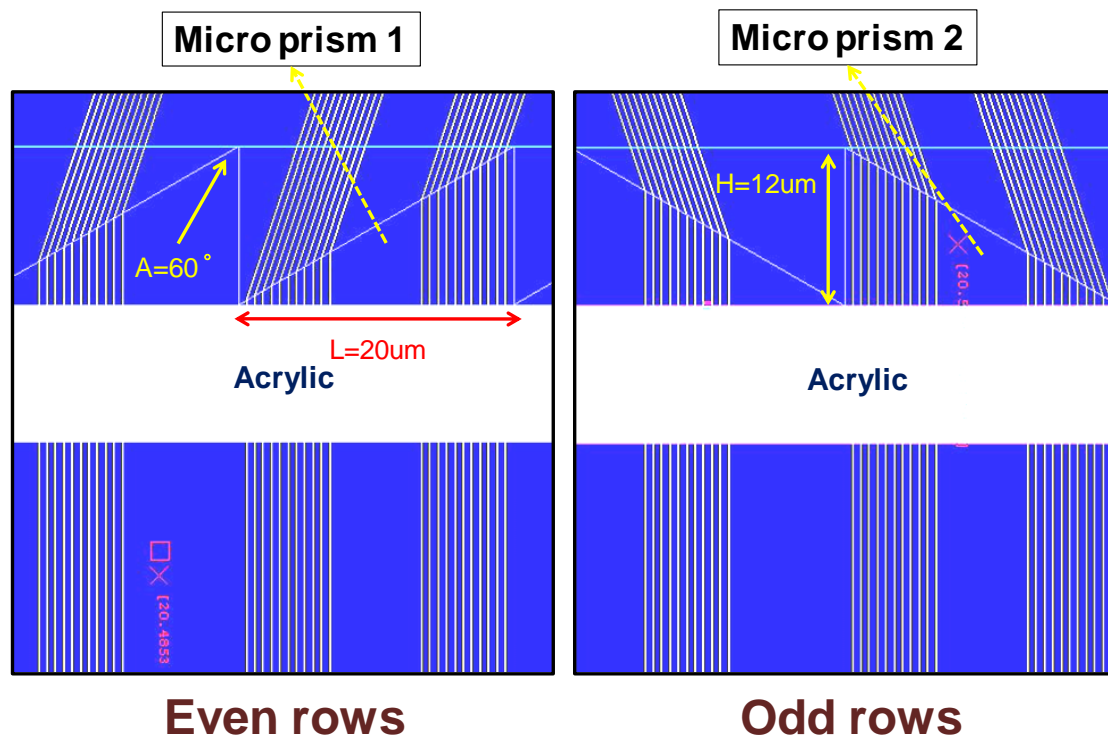
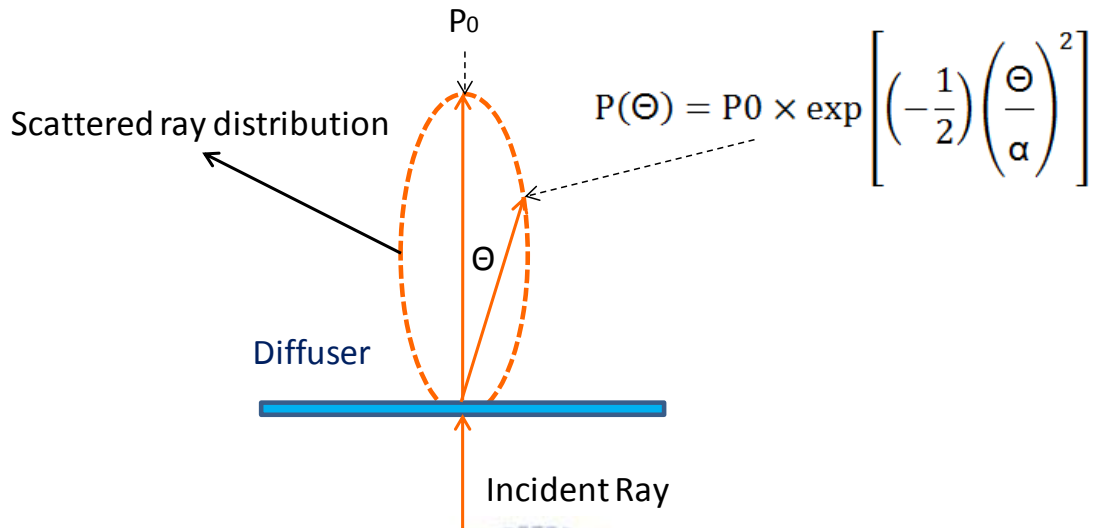


Fig. 4-12 Refraction on micro prism 1 and micro prism 2.

4.2.4 Diffuser

By using a 240Hz sequential LED backlight, a cylindrical lens and a dual directional prism, the proposed backlight produced four viewing zones sequentially. However, dark images were caused due to low viewing-zone uniformity and this issue was solved by adding an adequate diffuser. To optimize the diffuser, the Gaussian scattering angle (α) is defined in Fig. 4-13. A diffuser fabricating with a large α value had high average crosstalk and high viewing-zone uniformity. As mentioned in Sec. 2.1.1 if the average crosstalk is over 15%, 3D images are distorted [24]. In Sec. 2.1.2, if the viewing-zone uniformity is below 70%, dark images occur. Thus, in Fig. 4-14, when $\alpha = 8^\circ$, the average crosstalk is below 15% and the viewing-zone uniformity is 80%.. The four viewing zones light distribution is shown in Fig. 4-15. Therefore, the optimized α was 8° , and haze of the diffuser defined in Sec. 3.1.4 was 60%. Finally,

by utilizing the four components optimized above, the four-directional temporal backlight produced four viewing zones sequentially with acceptable average crosstalk and viewing-zone uniformity.



$P(\Theta)$: intensity or radiance in the Θ direction
 P_0 : strongest intensity or radiance in certain direction
 α : standard deviation of the Gaussian distribution, in degrees

Fig. 4-13 Diagram of Gaussian scattering phenomenon.

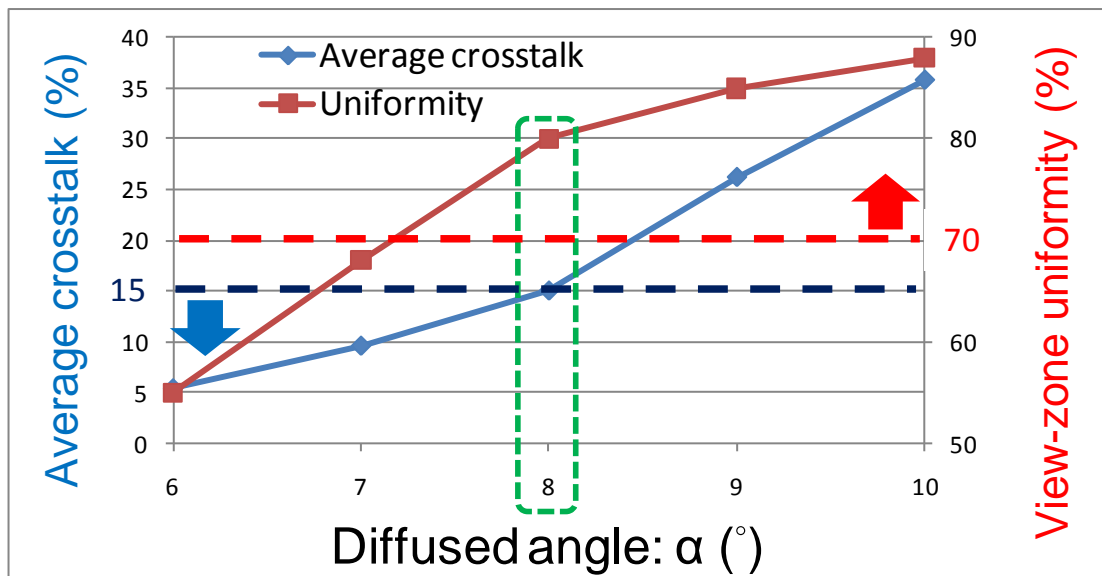


Fig. 4-14 Average crosstalk & viewing-zone uniformity vs. α .

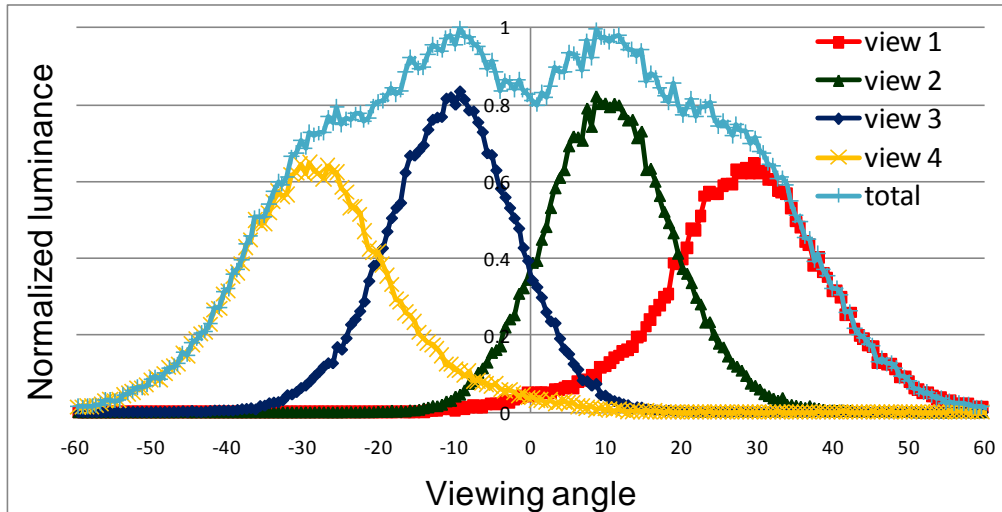


Fig. 4-15 Four-directional temporal backlight light distribution in simulation.

4.3 Summary

The four-directional temporal backlight was designed to produce four viewing zones sequentially, including a sequential LED plate, a cylindrical lens, a dual directional prism, and a diffuser. The optimized parameter values are shown in Tab. 4-1. The average crosstalk and the viewing-zone uniformity in the proposed backlight were 14.57% and 80%. Therefore, a 3D display using the proposed backlight produced clear and continuous 3D images.

LED plate	LED pitch (P)	4mm
	LED divergent angle (Θ)	$\pm 20^\circ$
Cylindrical lens	Curvature radius (R)	10mm
	Distance from LEDs (D)	12mm
Dual directional prism	Length (L)	20um
	Width (W)	4mm
	Height (H)	12um
	Obtuse angle (A)	60°
Diffuser	Diffused angle (α)	8°

Tab. 4-1 Optimized parameter values in four-directional temporal backlight.

Chapter 5

System Tolerances & Experimental Results

Before fabricating the proposed 3D display, system tolerances were evaluated to assure experimental results. Then, a spatial-temporal hybrid multi-view 3D display was fabricated by adding a multi-view parallax barrier above a four-directional temporal backlight. Finally, the ConoScope measured the proposed 3D display performance and compared results with the simulation model.

5.1 Tolerance of the Four-Directional Temporal Backlight

The four-directional temporal backlight had been optimized by simulation. However, because manufacture processes sometimes causes errors, fabrication results are easily different between simulation results. Thus, before experiment, tolerance of the backlight system is evaluated in this section.

5.1.1 Distance between Neighboring LEDs (P)

As mentioned in Sec. 4.2.1, the optimized P was 4mm for hot spots phenomenon. If $P < 4\text{mm}$, two viewing zones behind the cylindrical lens are close. So after adding the dual directional prism, the average crosstalk is over 15% and the uniformity between view 2 and view 3 is below 70%. Similarly, if $P > 4\text{mm}$, since angular difference between two viewing zones after the cylindrical lens is distant, the uniformity between view 1 and view 2 and the uniformity between view 3 and view 4 are below 70%. As shown in Fig. 5-1, the tolerance of P is below $\pm 0.25\text{mm}$. Light distributions of $P=3\text{mm}$, 4mm and 5mm are also shown in Fig. 5-2.

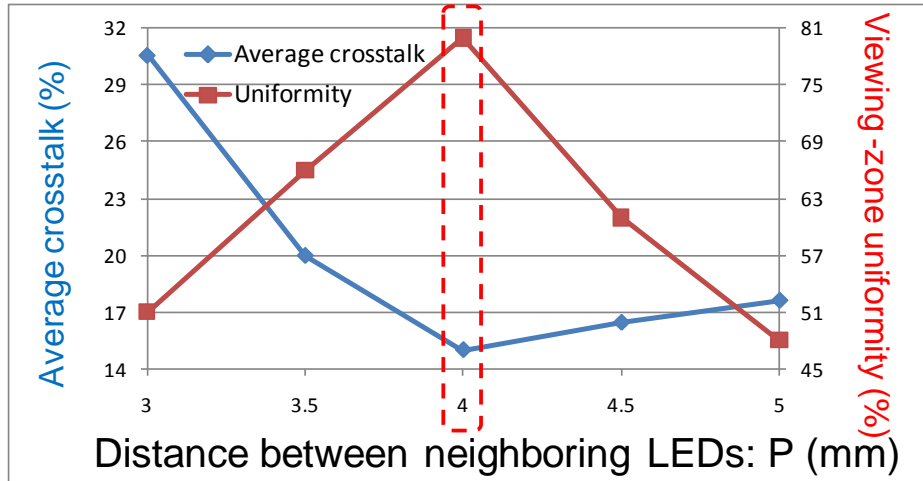


Fig. 5-1 Tolerance of distance between neighboring LEDs (P).

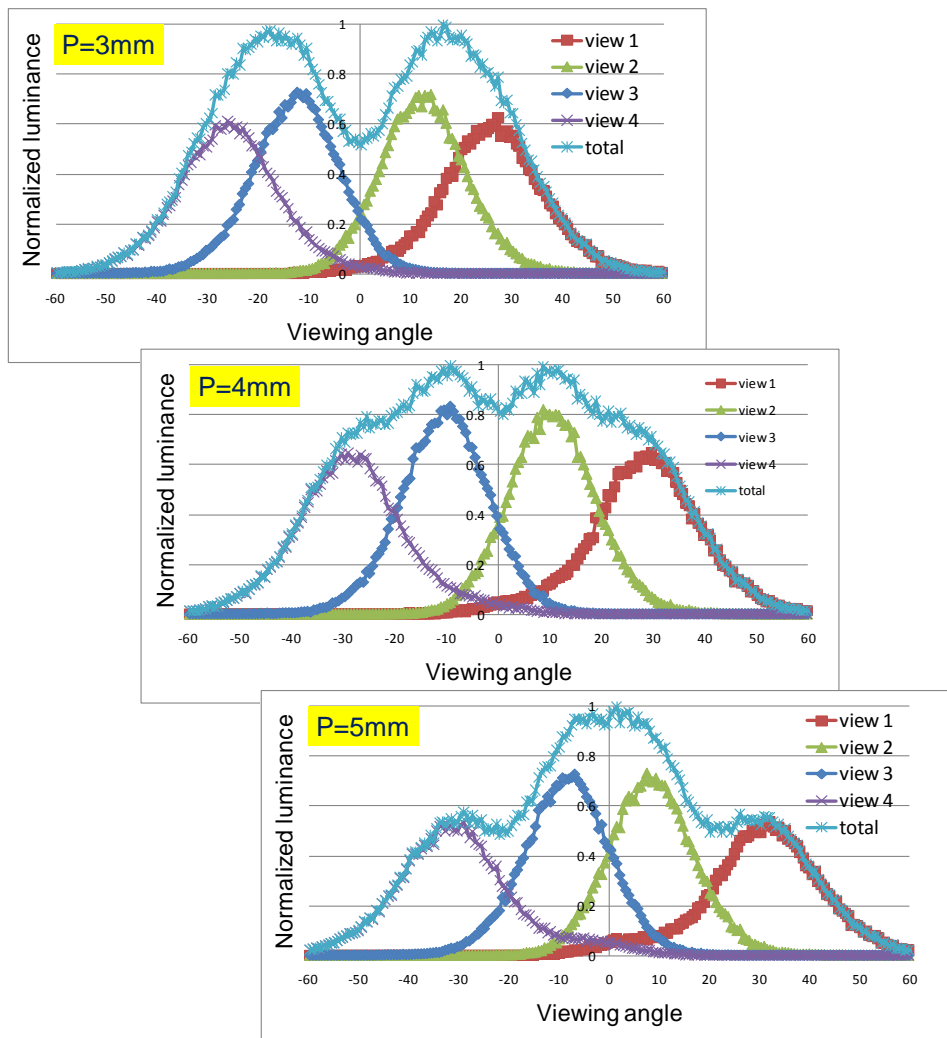


Fig. 5-2 Light distributions of P=3mm, 4mm and 5mm.

5.1.2 Divergent Angle of LEDs (Θ)

The divergent angle of white LEDs in simulation was $\pm 20^\circ$. In Fig. 5-3, if $\Theta < \pm 20^\circ$, angular difference between view 1 and view 2 and angular difference between view 3 and view 4 are close. So the uniformity between viewing zone 2 and viewing zone 3 is low. If $\Theta > \pm 20^\circ$, rays illuminating side of the cylindrical lens caused light leakage. So the average crosstalk was large. Thus in Fig. 5-4, the optimal Θ is $\pm 20^\circ$ and the tolerance of Θ is nearly $\pm 4^\circ$.

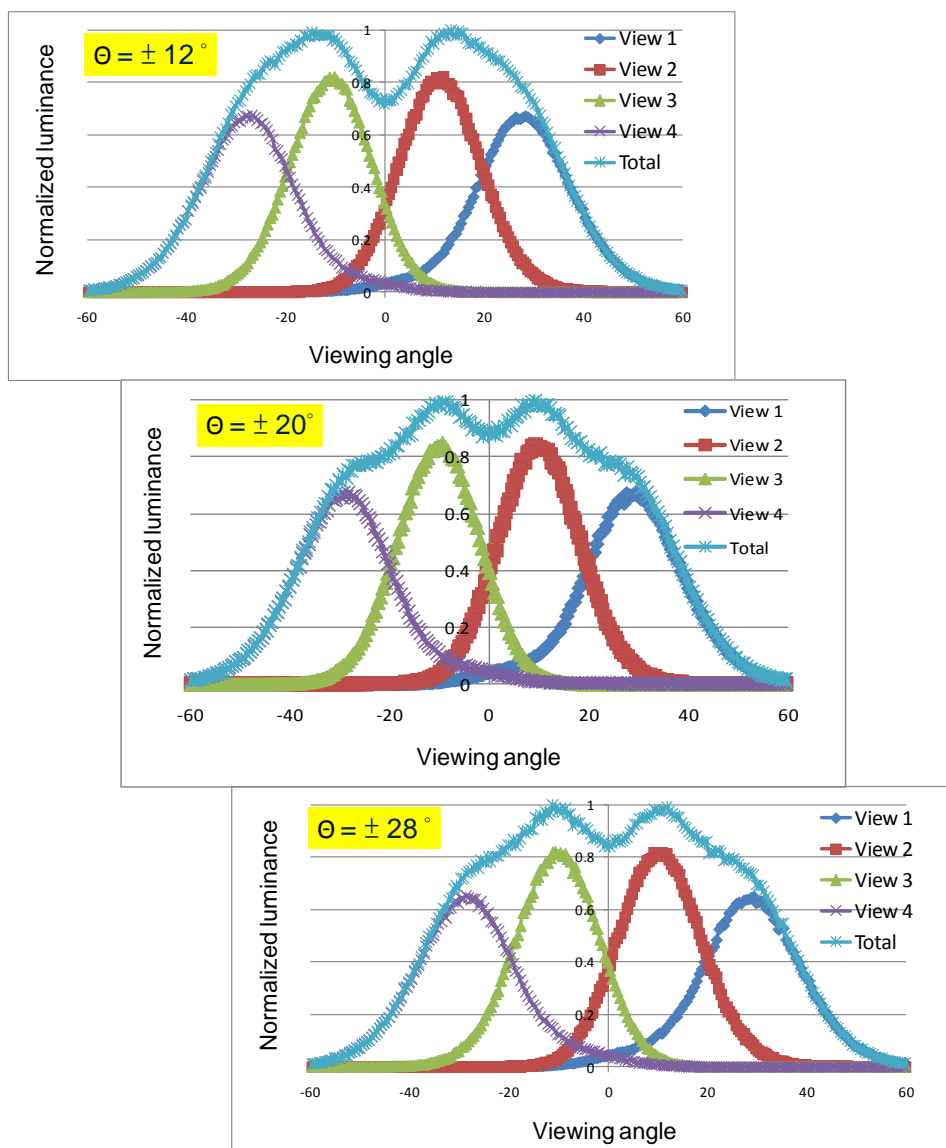


Fig. 5-3 Light distributions of $\Theta = \pm 12^\circ$, $\pm 20^\circ$ and $\pm 28^\circ$.

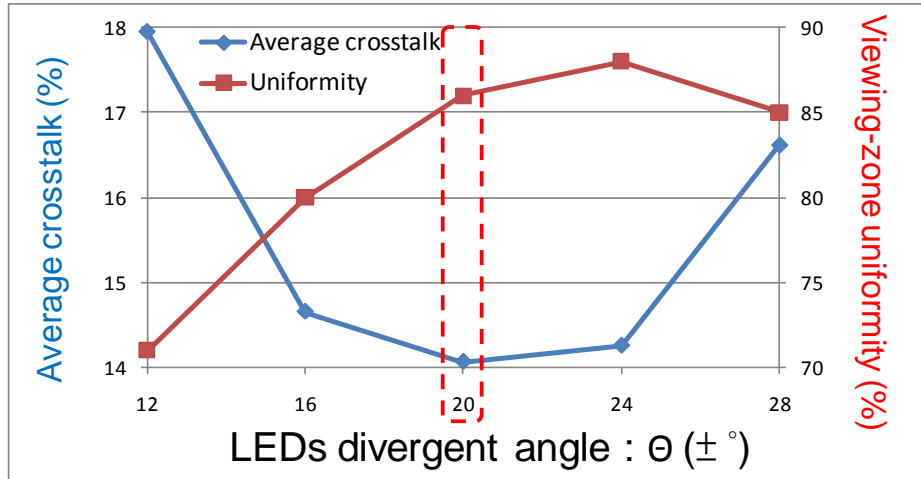


Fig. 5-4 Tolerance of LEDs divergent angle (θ).

5.1.3 Curvature Radius of Lens (R)

A lens fabricating in small curvature radius has large curvature, and a lens with large curvature separates lights well and produces low average crosstalk. Because the lens thickness in simulation was 10mm, the R min was 10mm. As shown in Fig. 5-5, if $R > 12\text{mm}$, the average crosstalk is much larger than 15%. Thus in fabrication, the tolerant R was $\pm 2\text{mm}$.

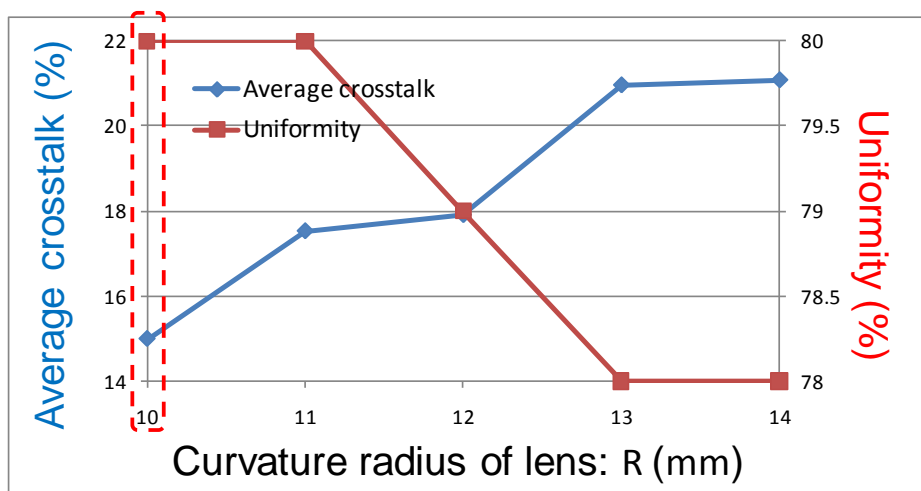


Fig. 5-5 Tolerance of lens curvature radius (R).

5.1.4 Distance between Lens and LEDs (D)

The distance between lens and LEDs related to light distributions. As shown in Fig. 5-6, view 2 and view 3 are close while $D > 12\text{mm}$. If $D < 12\text{mm}$, angular difference between view 1 and view 2 and angular difference between view 3 and view 4 are close. Both cases produced large average crosstalk and low uniformity. Therefore, in Fig. 5-7, the optimal D was 12mm and the tolerance of D is smaller than $\pm 1\text{mm}$.

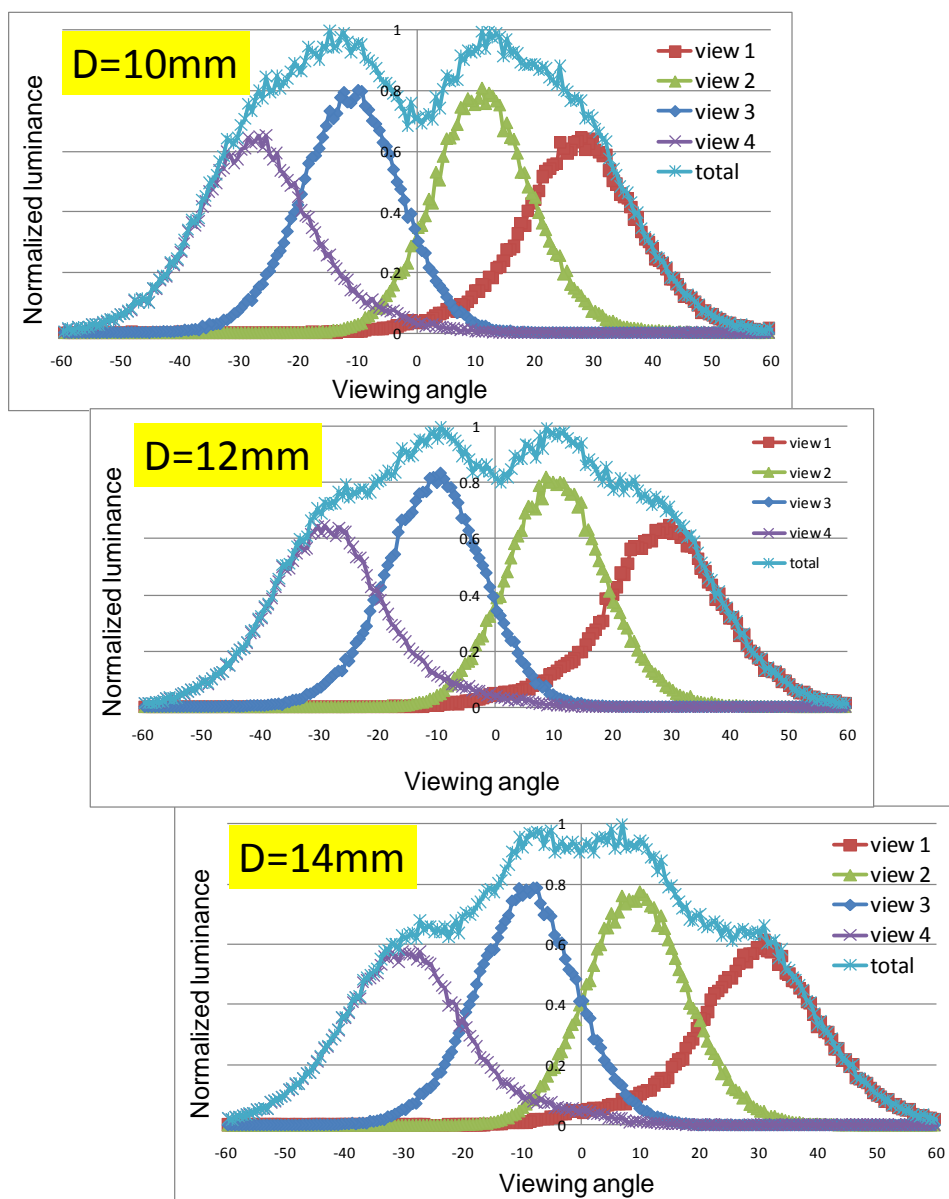


Fig. 5-6 Light distributions of D=10mm, 12mm and 14mm.

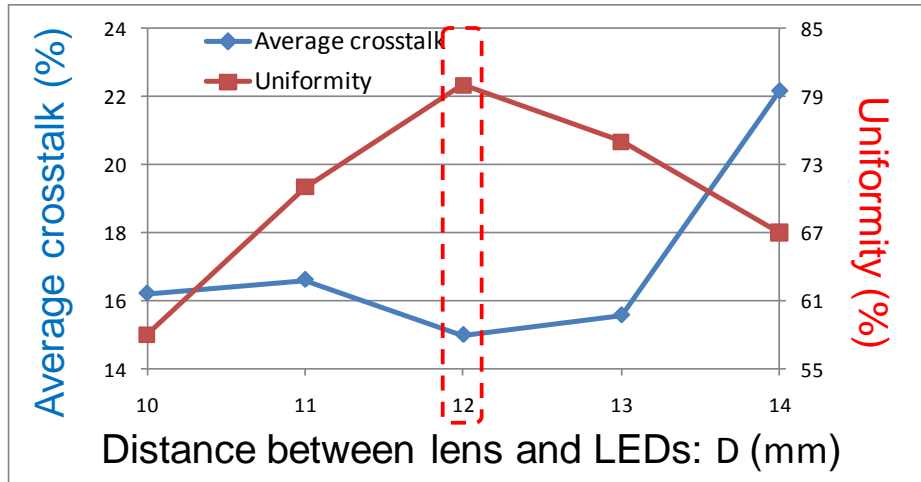


Fig. 5-7 Tolerance of distance between lens and LEDs (D).

5.1.5 Obtuse angle of dual directional prism (A)

The obtuse angle of dual directional prism determined the angular shift by refraction. In Fig. 5-8, the optimal A is 60° and the tolerance of D is $\pm 1^\circ$. As shown in Fig. 5-9, if $A < 59^\circ$, the angular shift phenomenon is so strong that the uniformity between view 2 and view 3 is lower than 70%. If $A > 61^\circ$, the angular shift phenomenon is weak. So view 2 and view 3 are close and the average crosstalk is over 15%.

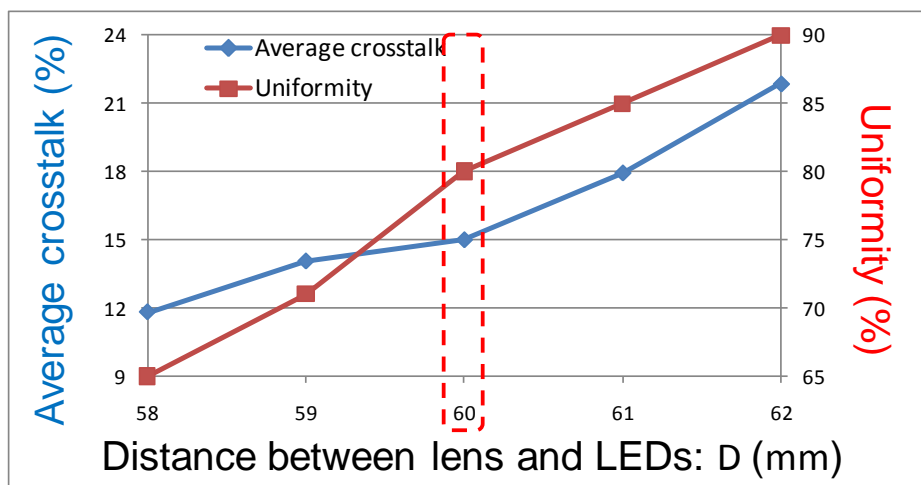


Fig. 5-8 Tolerance of obtuse angle in dual directional prism (A).

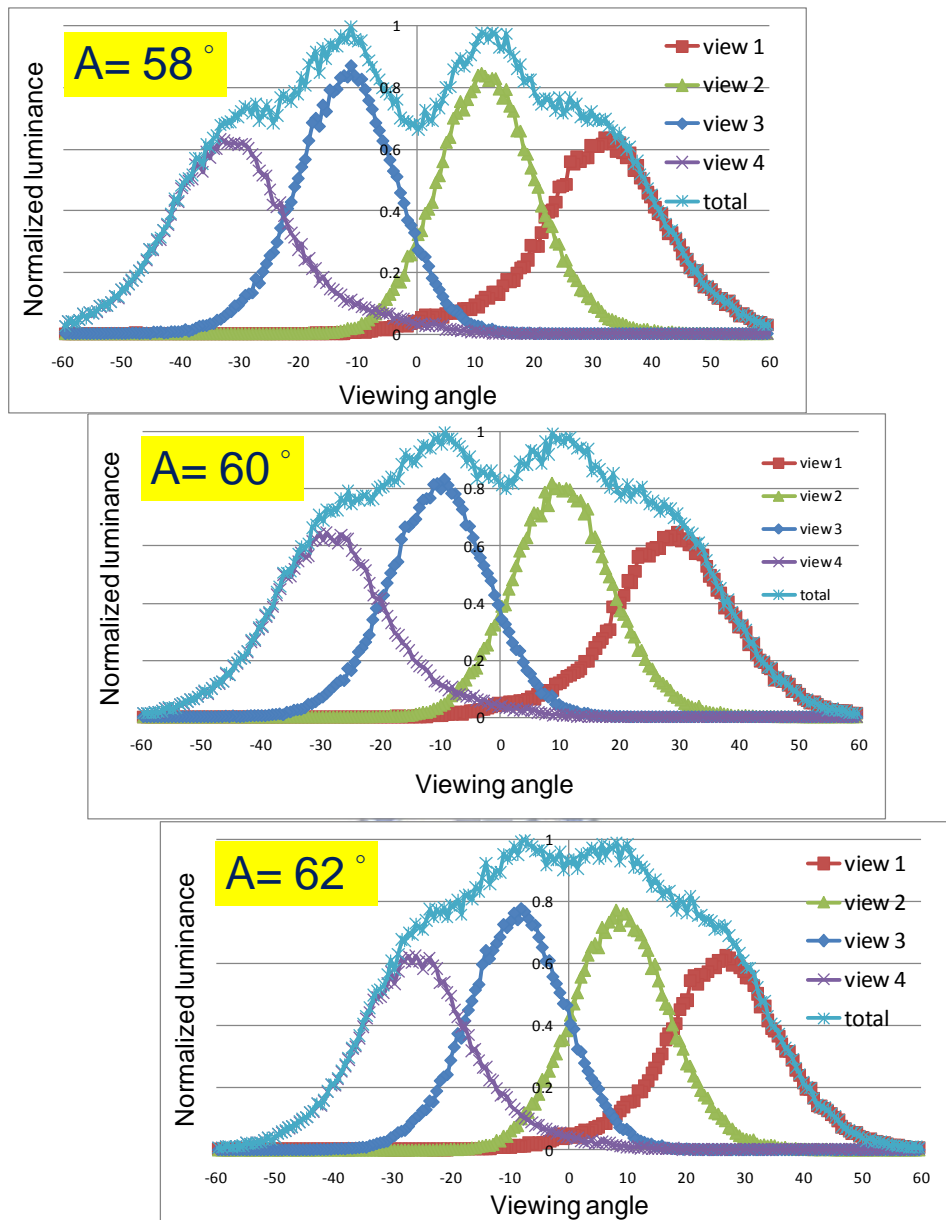


Fig. 5-9 Light distributions of $A=58^\circ$, 60° and 62° .

5.2 Demonstration of Four-Directional Temporal Backlight

The four-directional temporal backlight had been optimized in Chapter 4, including a 240Hz sequential LED plate, a cylindrical lens, a dual directional prism, and a diffuser. Each component in fabrication is shown in Fig. 5-10. The material of cylindrical lens was Polycarbonate (PC) by using Computer Numerical Control (CNC)

lathe. The micro prism was fabricated in Polymethylmethacrylate (PMMA) by wheel Machining and was divided by laser to construct the dual directional prism. The diffuser was particle-diffusing diffuser with Haze = 60%.

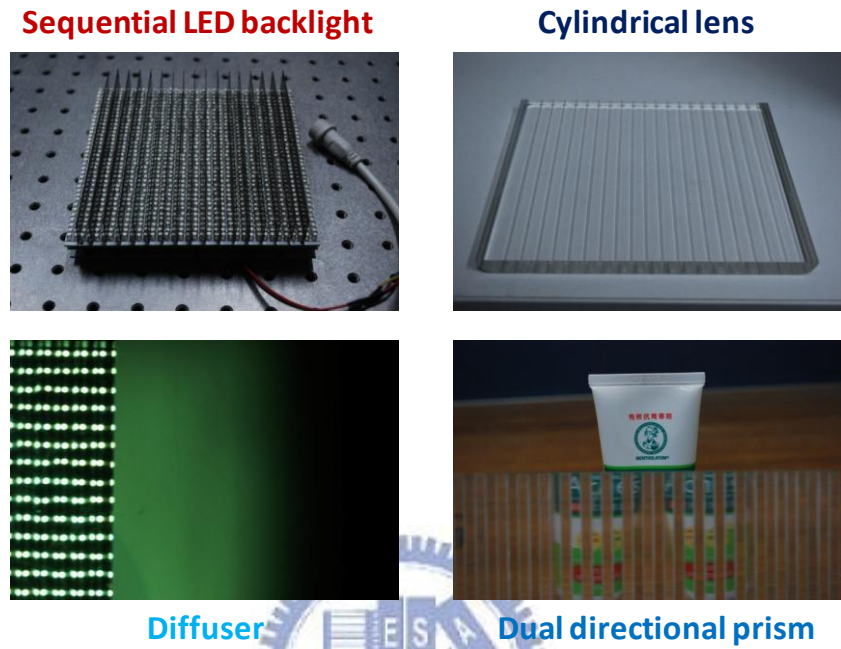


Fig. 5-10 Component implementations in four-directional temporal backlight.

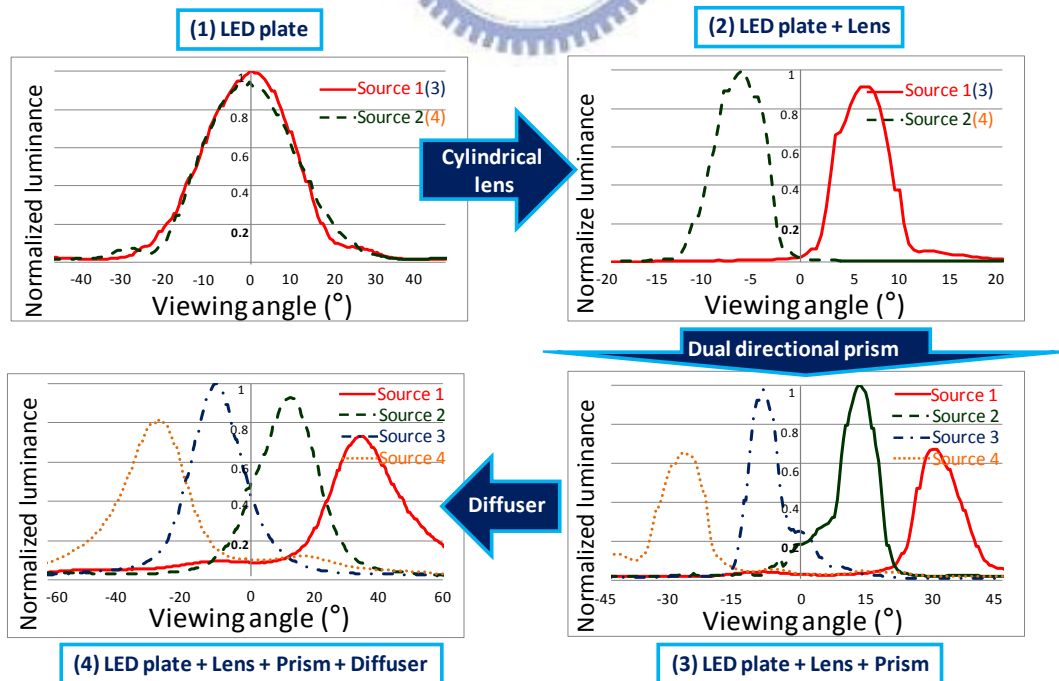


Fig. 5-11 Light distributions of four-directional temporal backlight.

Then, according to the optimized model, by combining above components, four viewing-zones are produced successfully, as shown in Fig. 5-11. The average crosstalk is 35% and the viewing-uniformity is 70%.

5.3 Spatial-Temporal Hybrid Multi-View 3D Display

The number of views divided by a multi-view parallax barrier was related to the viewing distance. As shown in Fig. 5-11, the FWHM (Full Width at Half Maximum) of each viewing zones is nearly 15° in the four-directional temporal backlight. Thus, in Fig. 5-12, different multi-view parallax barriers are designed according to 3D display specifications.

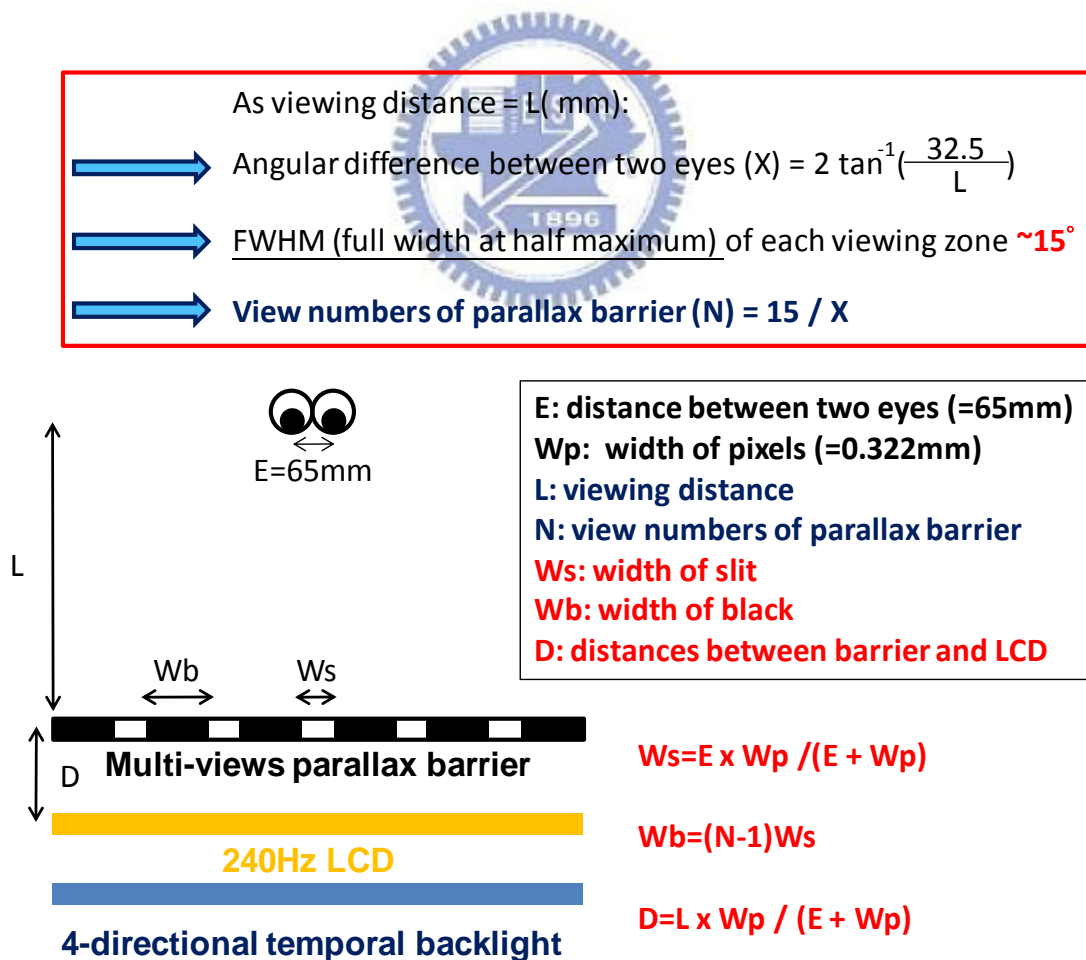


Fig. 5-12 Design of multi-view parallax barrier in the proposed 3D display.

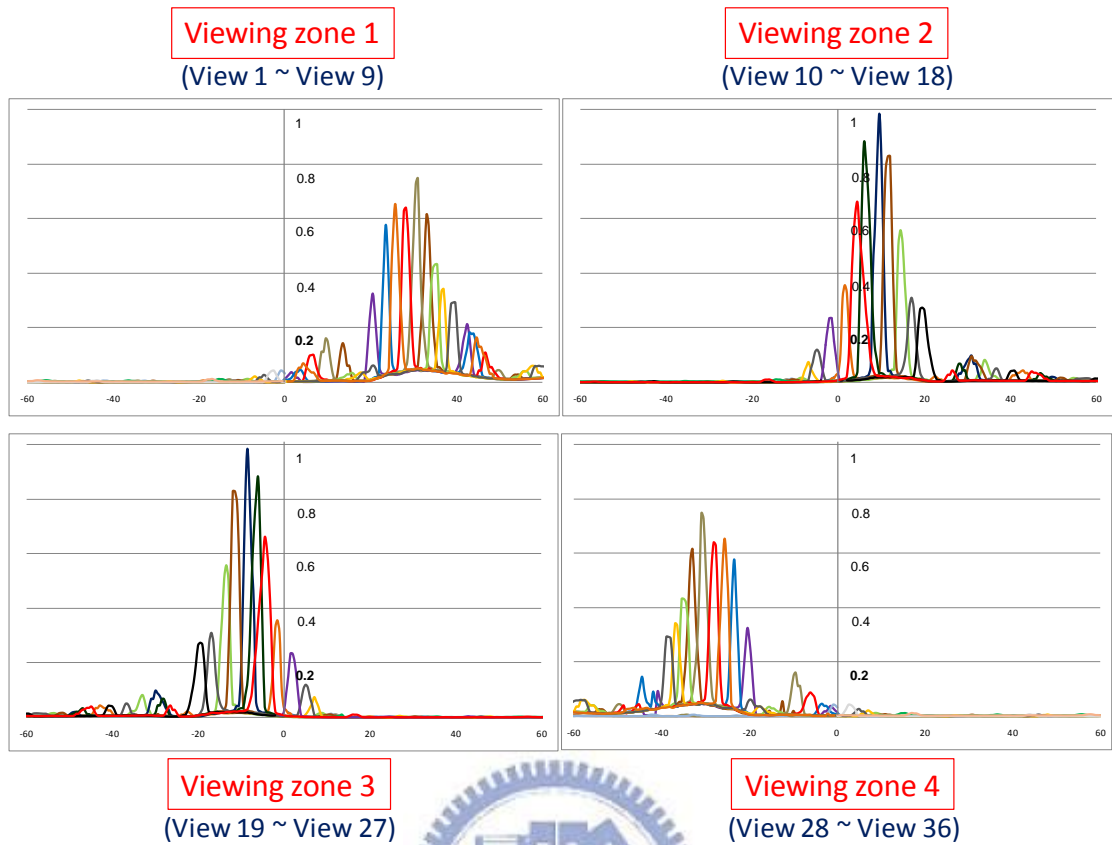


Fig. 5-13 Light distributions of spatial-temporal hybrid multi-view 3D display.

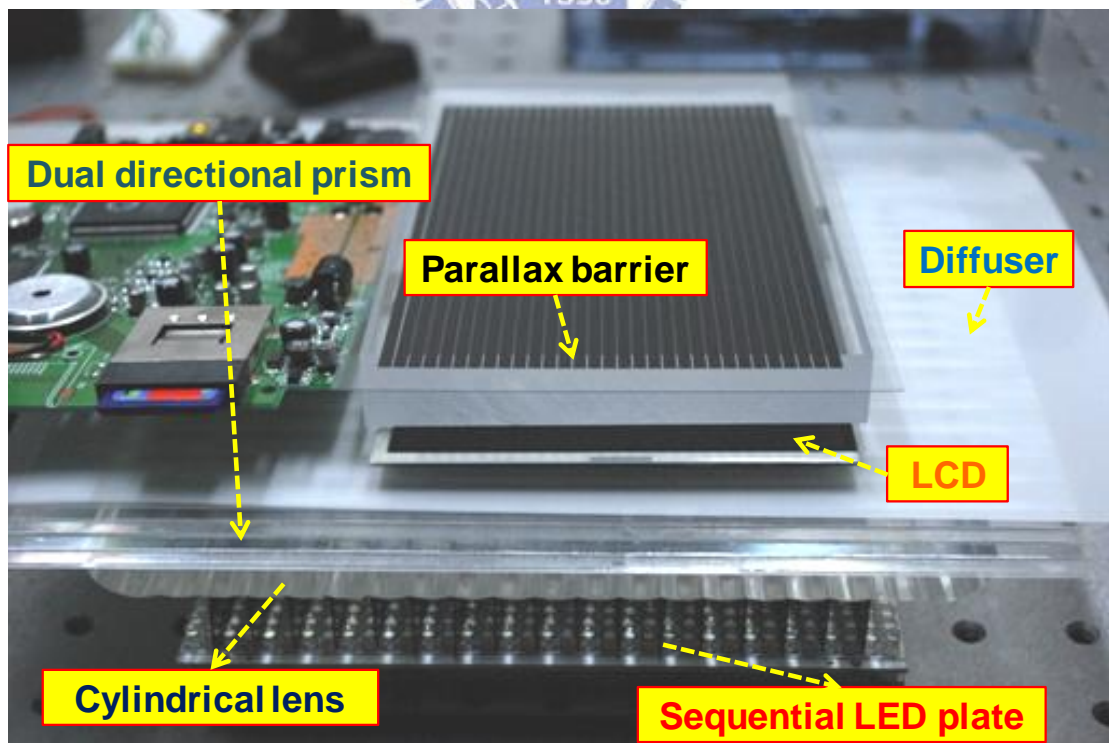


Fig. 5-14 Fabrication of spatial-temporal hybrid multi-view 3D display.

Fig. 5-13 shows the four viewing zones after adding a 9-view parallax barrier. The 9-view parallax barrier divides each viewing zone into 9 parts. Therefore, the number of views defined in Sec. 2.1.2 increased from 4 to 36. A spatial-temporal hybrid multi-view 3D display was implemented in Fig. 5-14. The number of views was 36 with $\pm 40^\circ$ viewing angle. Compared with the resolution and the light efficiency decreased to $1/36$ in 36-view spatial-multiplexed 3D displays, the resolution and the light efficiency only decreased to $1/9$ in the spatial-temporal hybrid multi-view 3D display. Because the LEDs were direct-emission, the four-directional temporal backlight was also usable to present uniform 3D images in large LCD.



Chapter 6

Conclusions and Future Works

6.1 Conclusions

3D displays are pursued through needing more natural images. Images containing three-dimensional coordinate information are necessary for humans to perceive real life images. Nowadays, stereoscopic displays are widely used in cinemas due to ease of fabrication and vivid stereoscopic visions. Nevertheless, auto-stereoscopic displays get popular because wearing eyeglasses is not required and multi-view. However, image resolution, light efficiency, number of views, and image uniformity in large LCDs are still drawbacks in existing auto-stereoscopic displays. Therefore, a 2D-multiplexed 3D display combining spatial-multiplexed and temporal-multiplexed techniques was proposed.

The proposed 3D display included a multi-view parallax barrier, a 240Hz LCD, and a four-directional temporal backlight. The four-directional temporal backlight, comprising a sequential LED plate, a cylindrical lens, a dual directional prism and a diffuser, produced four viewing zones sequentially with acceptable average crosstalk and viewing-zone uniformity. Then the parallax barrier divided each viewing zone to present multi-view 3D images. The comparisons between the proposed 3D display and existing 3D displays are shown in Tab. 6-1. Because of the four-directional temporal backlight, the proposed 3D display presented better resolution and light efficiency by four times than spatial-multiplexed 3D displays, and 3D images in large LCDs were uniform. Furthermore, by combining spatial-multiplexed and

temporal-multiplexed techniques, the proposed 3D display produced multi-view 3D images more easily than temporal-multiplexed 3D displays.

	<u>Number of views</u>	<u>3D image Resolution</u>	<u>Light efficiency</u>
<i>Parallax barrier 3D display (Sharp)</i>	2	1/2	1/2
<i>Lenticular lens 3D display (Philips)</i>	9	1/9	1
<i>Time division parallax barrier 3D display (Samsung)</i>	2	1	1/2
<i>Sided- sequential 3D display (3M)</i>	2	1	1
<i>Spatial-temporal hybrid 3D system</i>	36	1/9	1/9

Tab. 6-1 Comparisons between existing 3D displays and the proposed 3D display.

6.2 Future Works

A temporal backlight with multi-view parallax barrier was demonstrated for large panels with wide viewing angle and multi-view, but still kept acceptable 3D resolution and light efficiency. However, as mentioned in 5.2 and Fig. 6-1, the average crosstalk in the four-directional temporal backlight prototype was over 15% due to alignment between LEDs, lens, and prism. The distance between the LED backlight and the dual directional prism also caused vertical crosstalk, as shown in Fig. 6-2. Therefore, in Fig. 6-3, by covering the LED backlight with the dual directional prism to improve distance and alignment between the LED backlight and the dual directional prism. Therefore, four viewing zones will also be produced with low horizontal and vertical crosstalk.

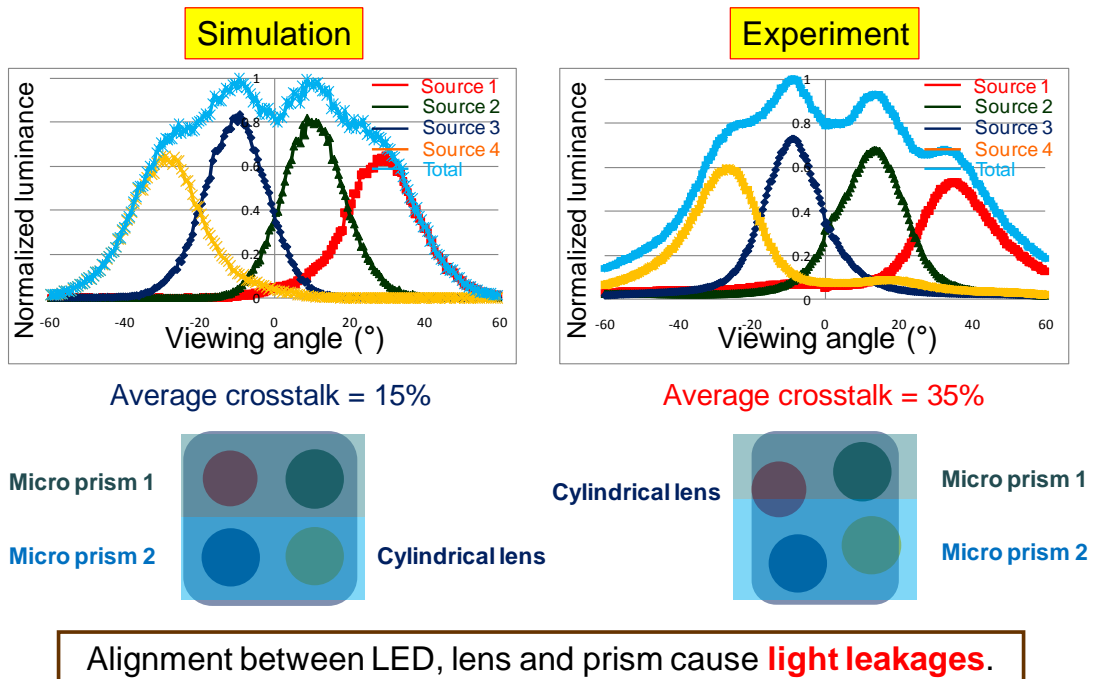


Fig. 6-1 Comparisons between simulation and experiment.

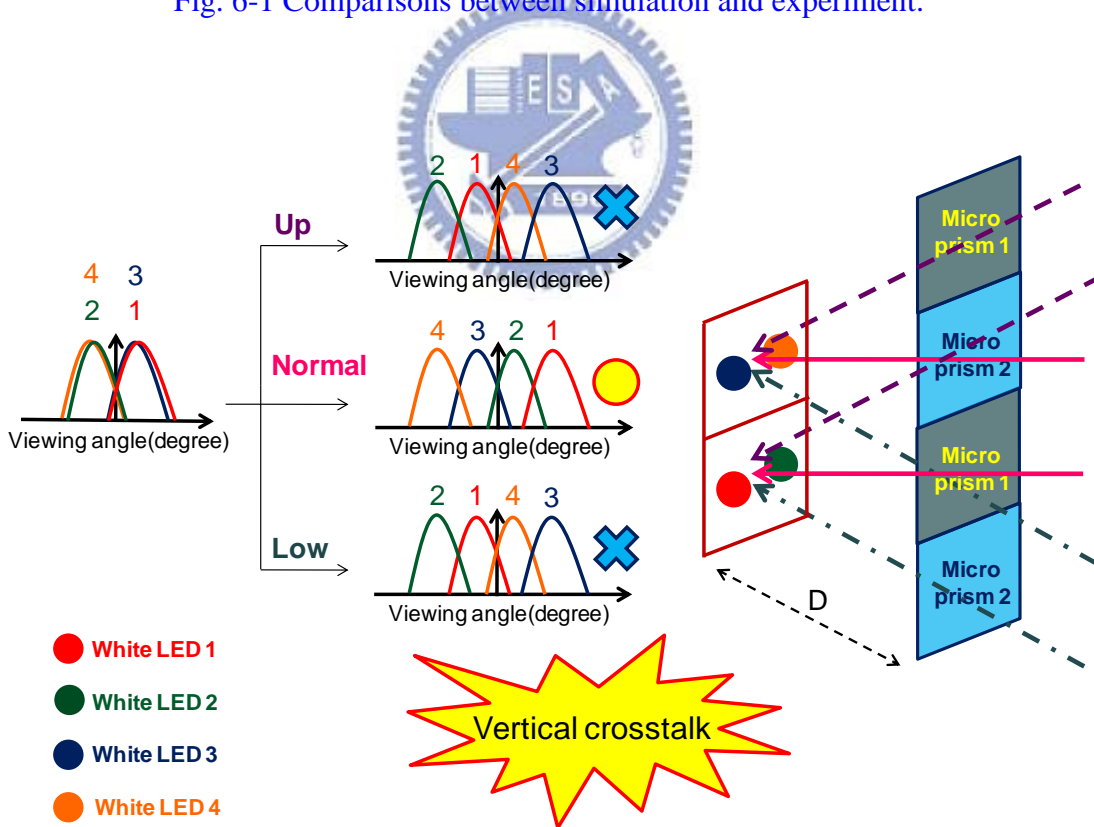


Fig. 6-2 Vertical crosstalk phenomenon.

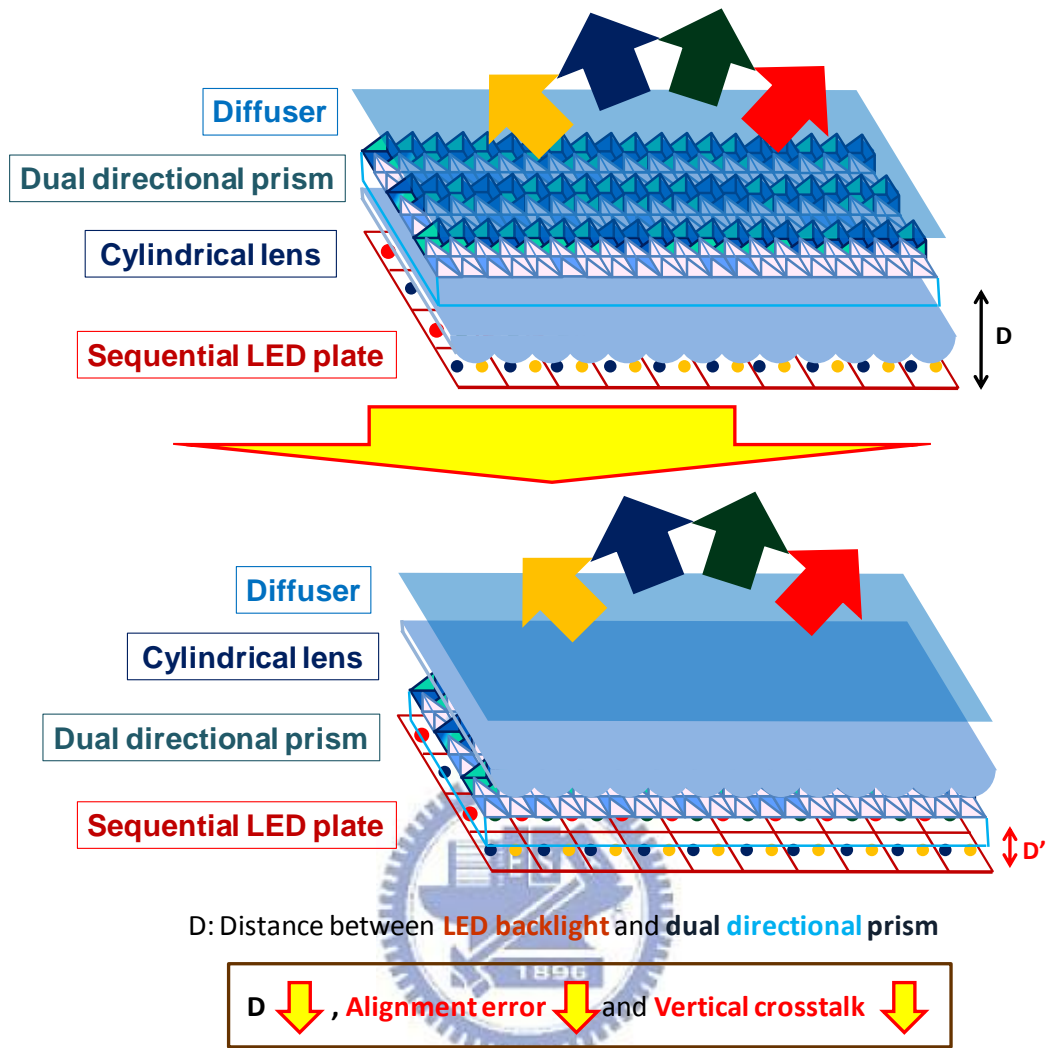


Fig. 6-3 Solutions to horizontal and vertical crosstalk.

Finally, because the proposed backlight produces four viewing zones sequentially at 240Hz, the LC response time in the proposed 3D display is also 240Hz. Therefore, the response time of LC must be lower than 2ms. One solution is using OCB (Optically Compensated Bend) mode LC [25] [26]. Because there is no backflow while changing state in OCB mode, the response time is from 5ms to 1ms. OCB mode also has ease of fabrication and wide viewing angle due to the self-compensated property. Another solution is Blue Phase mode LCD [27] [28]. Blue Phase is liquid crystal phase that appear in a temperature range between the cholesteric phase and the isotropic phase. The electro-optical response time at room temperature

is 0.1 ms for the stabilized Blue Phase. Furthermore, because the Blue Phase mode can make alignment layers, the mechanical pressure sensitivity and the manufacturing steps are reduced. In SID 2008, Samsung developed the first Blue Phase LCD with 240Hz refresh rate. Therefore, by combining the four-directional temporal backlight and the multi-view parallax barrier with an OCB LCD or a Blue Phase LCD, the spatial-temporal hybrid multi-view 3D display will be fabricated.

However, in the synchronization between the sequential backlight system and 240Hz LCD, if LEDs turn on too early or turn off too late, the spatial-temporal hybrid multi-view 3D display produces distorted 3D images due to the temporal crosstalk phenomenon, as shown in Fig. 6-4.

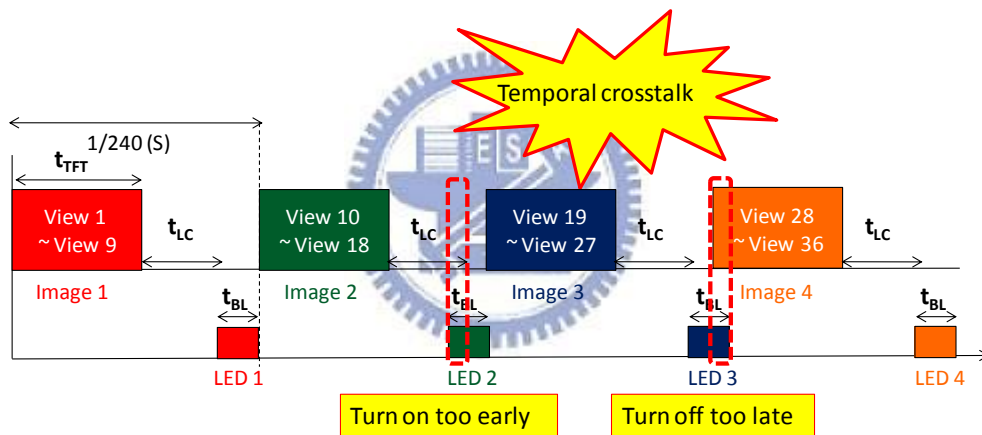


Fig. 6-4 Temporal crosstalk in the synchronization between the backlight and LCD.

Therefore, in Fig. 6-5, the t_{start} and t_{stop} are defined in the backlight synchronization. By adjusting values of t_{start} and t_{stop} , for example, the observer standing at position 2 can't see the frame 1 images and frame 3 images. So the temporal crosstalk is reduced and the 3D display present clear multi-view 3D images satisfied the simulation and experiment results mentioned before. However, periodic structure of the parallax barrier and the LCD cause moiré pattern in 3D images, as shown in Fig. 6-6. Therefore, the slanted parallax barrier design is also a vital work in the future.

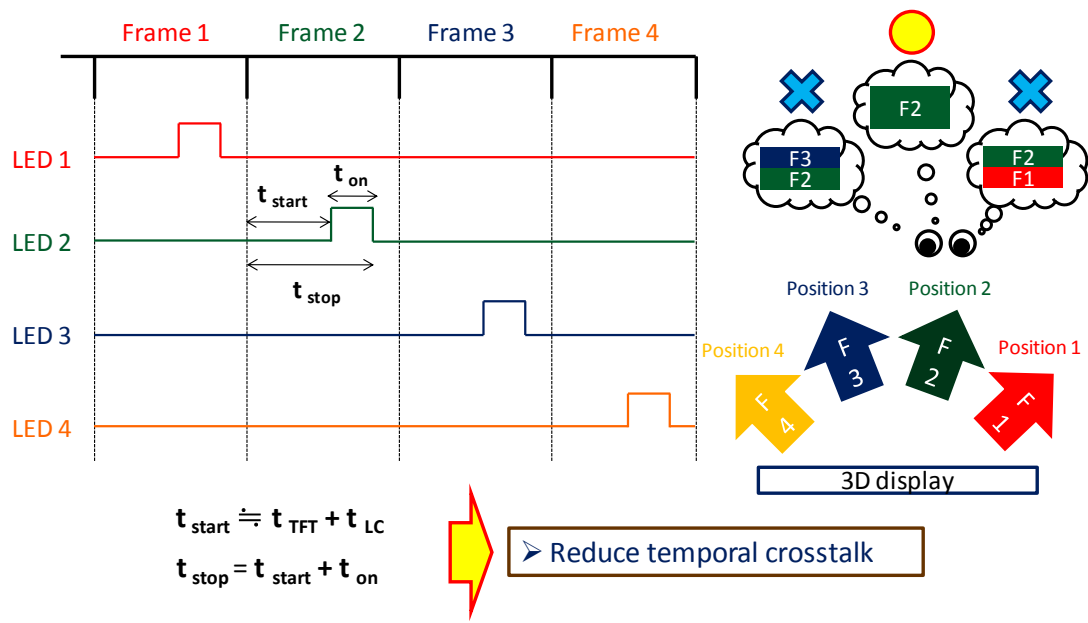


Fig. 6-5 Solutions to the temporal crosstalk phenomenon.



Fig. 6-6 Moiré phenomenon caused by the parallax barrier and the LCD.

References

- [1] Stereoscopic display and auto-stereoscopic display:
<http://images.sanhaostreet.com/News//2009/7/20090730171245662.jpg>.
<http://www.kingslingleyhotel.com/images/imax.jpg>.
- [2] C.Y. Hsu and Y. P. Huang, "Development and Researches of Real 3D Display Technologies," *Optical Engineering Quarterly* 98th, pp. 1-8, June, 2007.
- [3] W. Matusik and H. Pfister, "3D TV: A Scalable System for Real-Time Acquisition, Transmission, and Autostereoscopic Display of Dynamic Scenes." *International Conference on Computer Graphics and Interactive Techniques*, pp. 814-824, 2004.
- [4] H. Hong and M. Lim, "Determination of luminance distribution of autostereoscopic 3-D displays through calculation of angular profile," *Journal of the SID* 18/5, pp. 327-335, 2010
- [5] Y. C. Chang, C. Y. Ma, and Y. P. Huang, "Crosstalk Suppression by Image Processing in 3D Displays," *SID '10 DIGEST*, pp.124-127, 2010.
- [6] N. Holliman, "3D Display Systems," University of Durham, 3, Feb. (2005).
- [7] F. C. Lin, "A High Image Quality and Low Power Consumption Eco-LCD Using Stencil Field-Sequential-Color Method," NCTU PHD thesis, Aug. (2009).
- [8] H. W. Chuang, "Study of Front Illuminating Systems for Reflective Displays," NCTU master thesis, Jul. (2009).
- [9] D. Suzuki, T. Fukami, E. Higano, N. Kubota, T. Higano, S. Kawaguchi, Y. Nishimoto, K. Nishiyama, K. Nakao, T. Tsukamoto, H. Kato, "Crosstalk-Free 3D Display with Time-Sequential OCB LCD," *SID '09 DIGEST*, pp.428-431, 2009.
- [10] H. Kang, S. D. Roh, I. S. Baik, H. J. Jung, W. N. Jeong, J. K. Shin, and I. J. Chung, "A Novel Polarizer Glasses-type 3D Displays with a Patterned Retarder," *SID '10 DIGEST*, pp.1-4, 2010.
- [11] Q. H. Wang, Y. H. Tao, W. X. Zhao, and D. H. Li, "An Autostereoscopic 3D Projector Based on Two Parallax Barriers," *SID '09 DIGEST*, pp.619-621, 2009.
- [12] J.Y. Son, "Viewing Zones in 3-D Imaging Systems Based on Lenticular Parallax Barrier and Microlens Array Plates," *Journal of Applied Optics*, Vol. 43, No. 26, pp. 4985-4992, September 2004.
- [13] C. V. Berkel, A. R. Franklin and J. R. Mansell, "Design and Applications of Multiview 3D-LCD," *Design & Apps of 3D-LCD, Proc SID Euro-Display96*,

- pp109-112, 1996.
- [14] Q. H. Wang, Y. H. Tao, W. X. Zhao and D. H. Li, "Lenticular lens based 3D autostereoscopic liquid crystal display," Proc. of IDRC, Orlando, pp.306-308, (2008).
- [15] K. W. Chien and H. P. D. Shieh, "3D Mobile Display Based on Sequentially Switching Backlight with Focusing Foil," *SID '04 DIGEST*, pp.1434-1437, 2004.
- [16] Y. M. Chu, K. W. Chien, H. P. D. Shieh, J. M. Chang, A. Hu, and V. Yang, "3D Mobile Display Based on Dual Directional Lightguides," *IDMC '05 DIGEST*, pp.799-801, 2005.
- [17] K. W. Chien and H. P. D. Shieh, "Autostereoscopic Display Based on Directional Backlight with Fast Switching Liquid Crystal," *APPLIED OPTICS _ Vol. 45, No. 13 _ 1 May 2006*, pp.3106-3110, 2006.
- [18] T.Sasagawa, A.Yuuki, S.Tahata, O.Murakami, and K.Oda, "Dual Directional Backlight for Stereoscopic LCD," *SID '03 DIGEST*, pp.399-401, 2003.
- [19] J. C. Schultz, R. Brott, M. Sykora, W. Bryan, T. Fukami , K. Nakao, A. Takimoto, "Full Resolution Autostereoscopic 3D Display for Mobile Applications," *SID '09 DIGEST*, pp.127-130, 2009.
- [20] R. Brott, J. Schultz, "Directional Backlight Lightguide Considerations for Full Resolution Autostereoscopic 3D Displays," *SID '10 DIGEST*, pp.218-221, 2010.
- [21] S. E. Brigham, J. Schultz, "Directional Backlight Timing Requirements for Full Resolution Autostereoscopic 3D Displays," *SID '10 DIGEST*, pp.226-229, 2010.
- [22] H. J. Lee, H. Nam, J. D. Lee, H. W. Jang, M. S. Song, B. S. Kim, J. S. Gu, C. Y. Park and K. H. Choi, "A High Resolution Autostereoscopic Display Employing a Time Division Parallax Barrier," *SID '06 DIGEST*, pp.81-84, 2006.
- [23] H. P. Kuo, M.Y. Chuang, C. C. Lin, "Design correlations for the optical performance of the particle-diffusing bottom diffusers in the LCD backlight unit," *Powder Technology 192*, pp.116–121, 2009.
- [24] R. Kaptein and I. Heynderickx, "Effect of Crosstalk in Multi-View Autostereoscopic 3D Displays on Perceived Image Quality," *SID '07 DIGEST*, pp.1220-1223, 2007.
- [25] M. L. Lee, "Single Cell Gap Transflective TFT-LCDs Design based on PVA and OCB Modes," NTU master thesis, June. (2007).
- [26] Y. Ito, R. Matsubara, R. Nakamura, M. Nagai, S. Nakamura, H. Mori, and K. Mihayashi, "OCB-WV Film for Fast-Response-Time and Wide-Viewing-Angle LCD-TVs," *SID '05 DIGEST*, pp.986-989, 2005.
- [27] J. Cohen, "The Blue Phase of Cholesteric Liquid Crystals," http://guava.physics.uiuc.edu/~nigel/courses/569/Essays_2002/files/cohen.pdf.
- [28] Wikipedia: http://en.wikipedia.org/wiki/Blue_Phase_Mode_LCD.